

General Disclaimer

One or more of the Following Statements may affect this Document

- This document has been reproduced from the best copy furnished by the organizational source. It is being released in the interest of making available as much information as possible.
- This document may contain data, which exceeds the sheet parameters. It was furnished in this condition by the organizational source and is the best copy available.
- This document may contain tone-on-tone or color graphs, charts and/or pictures, which have been reproduced in black and white.
- This document is paginated as submitted by the original source.
- Portions of this document are not fully legible due to the historical nature of some of the material. However, it is the best reproduction available from the original submission.

**NASA TECHNICAL
MEMORANDUM**

NASA TM X-71856

NASA TM X-71856

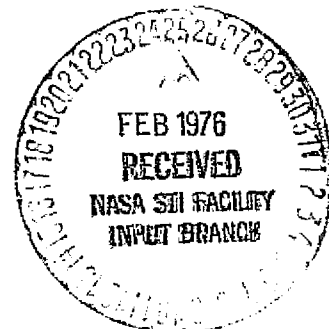
(NASA-TM-X-71856) ELECTROLYTIC HYDROGEN
PRODUCTION: AN ANALYSIS AND REVIEW (NASA)
70 p HC \$4.50 CSCL 10A

N76-17641

Unclas
G3/44 14156

ELECTROLYTIC HYDROGEN PRODUCTION
An Analysis and Review

by J. Evangelista, B. Phillips, and L. Gordon
Lewis Research Center
Cleveland, Ohio 44135
December 1975



1. Report No. NASA TM X-71856	2. Government Accession No.	3. Recipient's Catalog No.	
4. Title and Subtitle ELECTROLYTIC HYDROGEN PRODUCTION An Analysis and Review		5. Report Date December 1975	
		6. Performing Organization Code	
7. Author(s) John Evangelista, Bert Phillips, and Larry Gordon		8. Performing Organization Report No. E-8602	
		10. Work Unit No.	
9. Performing Organization Name and Address Lewis Research Center National Aeronautics and Space Administration Cleveland, Ohio 44135		11. Contract or Grant No.	
		13. Type of Report and Period Covered Technical Memorandum	
12. Sponsoring Agency Name and Address National Aeronautics and Space Administration Washington, D. C. 20546		14. Sponsoring Agency Code	
		15. Supplementary Notes	
16. Abstract <p>The potential advantages of hydrogen energy storage systems for electrical power generation is currently being assessed and recognized by many independent utilities, institutions, and agencies. The electrolysis of water to produce hydrogen is the favored near-term production concept in this energy storage system and consequently, a prime area to address for overall system improvements. The thermodynamics of water electrolysis cells is presented, followed by a review of current and future technology of commercial cells. The irreversibilities involved are then analyzed and the resulting equations assembled into a computer simulation model of electrolysis cell efficiency. The model is tested by comparing predictions based on the model to actual commercial cell performance, and a parametric investigation of operating conditions is performed. Finally, the simulation model is applied to a study of electrolysis cell dynamics through consideration of an ideal pulsed electrolyzer.</p>			
17. Key Words (Suggested by Author(s))		18. Distribution Statement Unclassified - unlimited	
19. Security Classif. (of this report) Unclassified	20. Security Classif. (of this page) Unclassified	21. No. of Pages	22. Price*

* For sale by the National Technical Information Service, Springfield, Virginia 22161

Table of Contents

I.	Introduction	1
II.	Thermodynamics	2
III.	Review of Current and Future Technology	9
	A. Introduction	9
	B. Electrolysis Cell Operating Parameters	12
	C. Electrolyser Corporation Ltd.	16
	D. Teledyne Isotopes	18
	E. Lurgi Apparate - Technik, GMBH	19
	F. Bamag Verfahrenstechnik GMBH	20
	G. Norsk Hydro Verksteder A-S	21
	H. Life Systems, Inc.	22
	I. General Electric	23
	J. Summary and Comparison of Electrolysis Cells	24
IV.	Modeling of Electrolysis Cell Efficiency	25
	A. Chemical Polarization	25
	B. Ohmic Losses	27
	C. Concentration Polarization	32
	D. Cell Voltage Summary	34
	E. Model Verification	39
V.	Electrolysis Cell Dynamics	41
VI.	Summary and Conclusions	44
	List of References	45
	Appendix - Computer Simulation Model	49

ELECTROLYTIC HYDROGEN PRODUCTION - AN ANALYSIS AND REVIEW

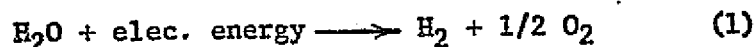
I. INTRODUCTION

The potential advantages of hydrogen energy storage systems for electrical power generation is currently being assessed and recognized by many independent utilities, institutions, and agencies. These energy storage systems consist of three major subsystems: production, storage/transmission, and utilization. The current hydrogen scenarios agree that thorough understanding of a high efficiency, low cost production subsystem is first priority for this energy storage system. The favored near-term approach is the electrolytic production of hydrogen. An initial attempt to understand and model the characteristics of electrolysis cells is the subject of this report.

This report attempts to analyze the inefficiencies encountered in electrolyzer operation. Following a discussion of the thermodynamics of electrolysis cell operation, current and near future technology of commercial units is reviewed. Information from manufacturers is then combined with some recent research efforts to form the basis of a mathematical representation of cell inefficiency. The model so constructed is tested and thus is used to predict cell performance characteristics under various conditions.

II. THERMODYNAMICS

In the electrolysis of water, a current is passed through an aqueous solution to produce hydrogen and oxygen:



The electrical energy is thereby converted into chemical energy as hydrogen with a change in enthalpy at 25°C and 1 atm of

$$\Delta H = 68,320 \text{ cal./g-mole}$$

The first law of thermodynamics for a steady-flow system is

$$Q - W_s = \Delta H \quad (2)$$

in which

Q = heat added to the system

W_s = useful work done by the system

For the electrolysis unit, the work term is the electrical energy input to the cell, and is given by

$$W_s = -n \mathcal{F} E \quad (3)$$

in which

$n = 2$, the number of electrons transferred,

\mathcal{F} = The Faraday constant = 96,500 coulombs/gm equiv.
= 23,074 cal/volt - gm equiv.

E = the electric potential applied to the cell, volts

Combining equations (2) and (3) gives

$$E = \frac{\Delta H - Q}{nF} \quad (4)$$

For the present, interest lies in the reversible case (i.e., cell operation at thermodynamic equilibrium) for which equation (4) becomes

$$E = \frac{\Delta H - Q_{rev}}{nF} \quad (5)$$

Since an electrolysis cell operates isothermally, from thermodynamics,

$$Q_{rev} = T\Delta S \quad (6)$$

So that

$$E_{rev} = \frac{\Delta H - T\Delta S}{nF} \quad (7)$$

The numerator of equation (7) is simply the change in the Gibbs free energy for the reaction, and at 25°C, 1 atm

$$\Delta G = \Delta H - T\Delta S = 56,690 \text{ cal/gmole}$$

The reversible cell potential is then

$$E_{rev} = \frac{\Delta G}{nF} \quad (8)$$

and at 25°C, 1 atm

$$E_{rev} = \frac{56,690}{2(23,074)} = 1.229 \text{ volts}$$

Equation (8) may be combined with the Gibbs-Helmholtz equation

$$-\Delta G + \Delta H = -T \frac{d\Delta G}{dT} \quad (9)$$

to give

$$-E_{rev} + \frac{\Delta H}{nF} = -T \frac{dE_{rev}}{dT} \quad (10)$$

In order to integrate this equation, the variation of ΔH with temperature is needed. Since ΔH is also a function of pressure, this equation is first written in terms of a standard state defined as pure components at 1 atm pressure. Denoting the standard reversible cell potential as E_o and the standard enthalpy change as ΔH° gives

$$E_o + \frac{\Delta H^\circ}{n\mathcal{F}} = T \frac{dE_o}{dT} \quad \text{for } p = 1 \text{ atm} \quad (11)$$

The dependence of E_o on temperature can be formulated thermodynamically based on the observed heat of reaction, ΔH° . For the electrolysis reaction, the observed heat of reaction expressed as a voltage is

$$\left(\Delta H^\circ / n\mathcal{F} \right) = 1.480V \quad @ 25^\circ C$$

If the heat capacity of water is taken as 1 cal/gm - $^\circ C$ and that of the gases H_2 and O_2 as 7 cal/g-mole $^\circ C$ (the value for an ideal diatomic gas) then the value of $\Delta H^\circ / n\mathcal{F}$ can be expressed as

$$\Delta H^\circ / n\mathcal{F} = 1.449 + 1.625 \times 10^{-4} T \quad (12)$$

in which the temperature, T , is to be expressed in $^\circ K$.

Combining equations (11) and (12), integrating and using the value of E_o at $25^\circ C$ (1.229 volts) gives a relationship between E_o and temperature

$$E_o = 1.449 + (1.877 - 1.625 \ln T) \times 10^{-4} T$$

a_{H_2} and a_{O_2} in with T in $^\circ K$ and ($p = 1 \text{ atm}$) (13)

For an electrolysis cell using a KOH solution as the electrolyte the reversible cell potential varies with pressure and KOH concentration according to the Nerst equation

$$E_{\text{rev}} = E_0 + \left(\frac{RT}{nF} \right) \ln \frac{P_{\text{H}_2} (P_{\text{O}_2})^{1/2}}{a_{\text{H}_2\text{O}}} \quad (14)$$

where

E_{rev} = reversible cell potential, volts

E_0 = standard reversible cell potential, volts,
was given in equation (13)

R = gas constant

P_{H_2} = pressure of H_2 produced, atm

P_{O_2} = pressure of O_2 produced, atm

$a_{\text{H}_2\text{O}}$ = activity of water in solution

The activity and pressure contributions to the reversible cell potential in equation (14) may be separated and simplified to

$$E_{\text{rev}} = E_0 + \frac{3RT}{2nF} \ln P - \frac{RT}{nF} \ln a_{\text{H}_2\text{O}} \quad (15)$$

since the oxygen and hydrogen are generated at the same pressure (the cell operating pressure, P atm). With $R=1.987 \text{ cal/gmol}^\circ\text{K}$ this becomes

$$E_{\text{rev}} = 1.449 + (.646 \ln P + 1.877 - 1.625 \ln T - 0.431 \ln a_{\text{H}_2\text{O}}) \times 10^{-4} T \quad (16)$$

It remains to express the activity of water, $a_{\text{H}_2\text{O}}$, in terms of KOH concentration. Using the data of Costa and Grimes (ref. 1) with x equal to the weight fraction KOH in solution,

$$E_{\text{rev}} = 1.449 + [.646 \ln P + 1.877 + 2.7 x^2 - 1.625 \ln T] \times 10^{-4} T \quad (17)$$

Equation (17) is the desired expression for the reversible cell potential in terms of pressure, temperature and electrolyte concentration. An actual electrolysis cell must operate at a cell potential of at least this value. It is instructive to return at this point to equations (2) and (3) to consider actual (not reversible) operation.

Combining equations (2) and (3) gives

$$Q = \Delta H - n F E \quad (18)$$

For any set of conditions (P, T, X), the enthalpy change is fixed since enthalpy is a state property. The cell potential,

E, however, depends upon cell design parameters, approaching E_{rev} for a well-designed system. The actual cell potential required is always greater than the reversible cell potential corresponding to the same conditions of pressure, temperature and electrolyte concentration. For reversible operation, Q is a positive quantity over the range of interest since the enthalpy change is greater than the Gibb's free energy change, ΔG , which by equation (8) is the same as $nF E$. As the operation becomes more irreversible, the cell potential increases thereby decreasing Q. Eventually, a point is reached where Q vanishes and no heat need be added to the system. This is called thermoneutral operation, and by equation (18), corresponds to a cell potential

$$E_t = \frac{\Delta H}{nF} \quad (19)$$

in which E_t is the thermoneutral cell potential. For even greater irreversibility of operation, Q becomes negative. That is, in reversible operation heat is required, but cell inefficiency leads eventually to operation requiring cooling.

Electrolysis cell thermal efficiency is always calculated based on a comparison of the actual cell potential with the cell potential for thermoneutral operation:

$$\eta = \frac{E_t}{E} \times 100 \quad (20)$$

The thermoneutral cell potential, E_t , is used in preference to the reversible cell potential, E_{rev} , since the former represents the total energy requirement of the cell (ΔH), whereas the latter corresponds to only that portion of the energy requirement which must be supplied as electrical work and not as heat (ΔG). This is evident from equations (8), (18) and (19).

Since water enters the system pure and not in combination with the potassium hydroxide, the ΔH value is not dependent upon KOH concentration. The effect of pressure on ΔH for this operation is rather small and neglecting this leads to the conclusion that ΔH and ΔH° are equal. Using this in combination with equations (12) and (19) leads to

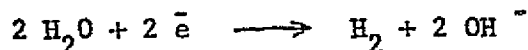
$$E_t = 1.449 + 1.625 \times 10^{-4} T \quad (21)$$

Equations (20) and (21) may be used to calculate the efficiency of an electrolysis cell. Since E can be less than E_t , the efficiency can be greater than 100% but operation in this range has yet to be demonstrated.

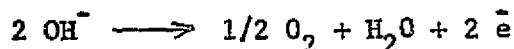
III. REVIEW OF CURRENT AND FUTURE TECHNOLOGY

III A. INTRODUCTION

An electrolysis cell for the production of hydrogen from water consists of an electrolyte, usually an aqueous basic solution, circulating between two electrodes. A membrane prevents the generated hydrogen and oxygen gases from mixing, and separates the cell into anolyte and catholyte chambers, while allowing ion transfer between the two. In a basic solution, the cathode reaction is



and oxygen is produced at the anode



The above expressions are overall reactions with no attempt being made to describe the still unsettled question of intermediates. The anode and cathode reactions combine to give a production of one mole of hydrogen plus one-half mole of oxygen from one mole of water. A basic solution is used in preference to pure water so as to increase the conductivity of the solution. This could also be accomplished using an acidic solution but the corrosion problems would be more severe.

The earliest electrolysis cells were unipolar tank-type cells wherein a single cell could contain several electrodes, each of a

fixed polarity. The anodes and cathodes of the cell are separated by one or more membranes so as to prevent mixing of the hydrogen and oxygen gases produced. The most common present-day cell is of the bipolar type. In this arrangement, each electrode serves a dual role as anode and cathode. That is, the plate that serves as the anode for one cell also constitutes the cell wall and is the cathode for the adjacent cell. The cells are joined together to form a pack and pressed together between end electrodes which are charged by a direct current source. The result is a design physically resembling a filter press and these units are commonly referred to as bipolar filter press electrolyzers. Both tank-type and filter press designs are described by Mantell (ref. 2).

Considerable research was performed in the 1960's on defining the operating characteristics of water electrolyzers. The Allison Division of General Motors (ref. 3) conducted a detailed investigation of the effects of current density, pressure and electrolyte velocity on cell performance using 6N KOH electrolyte at 75°C in a bipolar filter-press design. They also conducted testing and evaluation of materials for electrodes and membranes, as part of a study which encompassed all aspects of the design of an energy depot electrolysis system. Weight and mobility were established as important criteria in this design. In contract, the study performed

by Allis-Chalmers (ref. 4) considered low capital investment as the primary goal. This latter study was more restrictive but resulted in technology later applied commercially by Teledyne Isotopes. The thermodynamics and economics of the Allis-Chalmers investigation was presented in the classic work by Costa and Grimes (ref. 1).

The design and construction of industrial water electrolyzers was reviewed by Chapman (ref. 5) in 1965. More recently, Stuart (ref. 6) surveyed current operating performance of commercial units. Gregory's treatise on the hydrogen economy (ref. 7) provides a good review of current and advanced concepts and a more thorough review by the same author appears as part of an ONR project report (ref. 8). Another recent review of water electrolysis was motivated by the need for an energy storage device (ref. 9). The latter is a particularly good source for a discussion of the many ways in which efficiency is defined in describing electrolyzer performance. A survey of water electrolyzers for oxygen generation has also been performed (ref. 10) for their importance in spacecraft life-support systems.

The present summary of currently available and future generation electrolyzers has been compiled based on material found in the aforementioned reviews together with information received directly from a

few commercial manufacturers of large-scale electrolytic hydrogen equipment (refs. 11, 12, 13, 14, 15).

III B. ELECTROLYSIS CELL OPERATING PARAMETERS

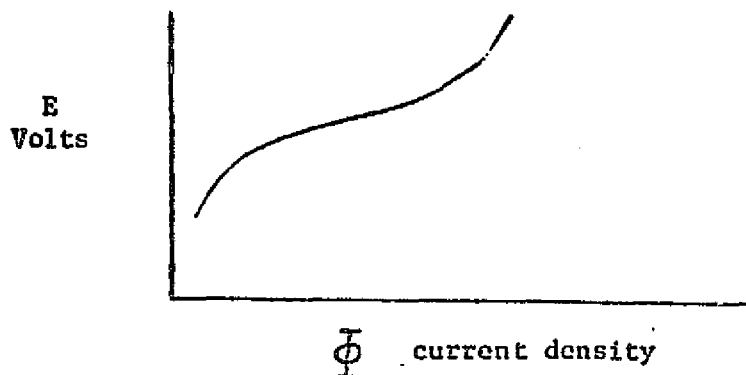
The thermodynamic reversible cell potential of an electrolysis cell using KOH electrolyte is given in equation (17) as a function of pressure, temperature and KOH concentration. Actual electrolysis cells require a greater cell potential (over voltage) due to the losses which occur in the cell. These losses consist of polarization at the electrodes, concentration polarization in the electrolyte solution, and ohmic losses in the cell. The losses in the cell depend upon the above mentioned operating parameters together with such cell design parameters as electrode spacing and electrolyte velocity. The cell design parameters will be considered in a later section of this report.

Electrolyzers are usually operated in the range 70-85°C with operation at the upper end of this range requiring somewhat higher pressures in order to minimize vaporization of the electrolyte. Both from a thermodynamic and kinetic viewpoint, higher operating temperatures are beneficial in reducing cell voltage requirements, and at least one manufacturer (ref. 12) is actively engaged in

developing new materials which will allow operation at temperatures above 120°C while maintaining cell integrity.

The effect of pressure on cell performance has been investigated (refs. 2, 3, 4, 16) with somewhat varying results. The reversible thermodynamic cell potential increases slightly as pressure is increased, but due to the reduction in bubble volume, there is a compensating reduction in the over-voltage. This point will be discussed in more detail later for the case of solid electrodes. The use of porous electrodes to some extent offsets the effect of bubbles on cell performance but there are structural problems associated with using them at high pressure. It is to be noted that Teledyne Isotopes uses porous electrodes successfully at 70 psig.

An important operating parameter which does not appear in equation (17) is the current density. Basically, the greater the current density, the more inefficient the cell. A typical plot of cell efficiency vs current density appears below:



The first steep portion of this curve is due to activation polarization at the electrodes; the steady climbing is a result of ohmic losses in the cell; the second steep section indicates the approach to the limiting current density, that is, the current density corresponding to the maximum mass transfer rate consistent with the given cell configuration and operating conditions.

The magnitude of the activation polarization term is dependent upon electrode material. For large industrial requirements, noble metals are too expensive. Nickel or nickel-plated steel is commonly used for the anode due to its availability, low cost, corrosion-resistance in KOH solution and low activation over-potential characteristics. Electrode performance is improved by increasing the effective surface area, thereby reducing the effective current density while maintaining cell size and current. All commercial manufacturers make use of this phenomenon in their design.

The predominant effect of electrolyte concentration on cell potential occurs due to the ohmic resistance of the electrolyte solution. Therefore, the cells using KOH solution as the electrolyte generally use 25-30% by weight KOH, thereby maximizing the conductivity of the solution. Electrolyte concentration also affects the rate of corrosion of cell components as well as the vapor pressure of the solution. This latter fact is exploited in a static feedwater design (ref. 17).

All of the operating parameters discussed above affect cost and in each case, a variation to increase the efficiency (and hence decrease the operating cost) of an electrolysis cell also increases the capital cost (and therefore the fixed cost). Depending upon cell configuration and design as well as economic factors, there is then an optimum choice of the operating parameters which minimizes the sum of operating and fixed costs.

The manner in which the operating parameters affect cost has been fairly well established. Higher temperatures increase efficiency thereby decreasing operating cost but the increased corrosion rate results in an increased maintenance and replacement cost. As previously described, increasing the cell pressure increases the efficiency but again at the expense of increasing the capital cost because of the thicker wall construction and safety apparatus required.

In order to discuss the relationship between current density and cost, it must be made explicit as to whether one is concerned with cost on an annual basis or cost per unit quantity of hydrogen produced. Consider, first of all, cost on an annual basis. As current density is increased, operating costs also increase due to a combination of increased current and increased cell potential.

Capital costs don't change and the resulting sum of fixed and operating costs increases monotonically with increasing current density. However, if cost per unit quantity of hydrogen produced is considered, an increase in current density still causes an increase in the operating costs due to reduced efficiency, but since the hydrogen generation rate is proportional to the current (and hence to the current density) the fixed cost is inversely proportional to current density. There is some value of current density which minimizes the sum of these costs.

III C. ELECTROLYSER CORPORATION LTD.

The Stuart Cell manufactured by the Electrolyser Corporation is a tank type unit with steel electrodes, the anode being nickel plated. It operates at about 160°F and a pressure just exceeding atmospheric (10"WG) using a 28% KOH solution as the electrolyte. The cell voltage is 2.04 v and the power consumption 128 kwhr DC per thousand cubic feet of hydrogen. The size of an individual cell varies from the 4000 amp unit which produces 63.6 ft³ H₂/hr to a 22,000 amp unit producing 349.8 ft³ H₂/hr. Larger requirements are handled by connecting individual cells in series. Electrolyser also markets packaged hydrogen generators producing anywhere from 20 to 1000 cubic feet of hydrogen per hour.

The tank type electrolyzer has several advantages over the bipolar filter press design. It uses fewer, less expensive parts

and since construction is modular, repair or replacement of a single cell can be accomplished by simply removing the defective cell via electrical connections. In a filter press type unit, the whole unit must be disassembled if a single cell diaphragm requires replacement.

The tank type cell of course also has its disadvantages. Due to construction, it operates at rather low current densities and generally requires greater floor space than a bipolar filter press unit. Tank type cells are also restricted with regard to operating temperature because of their size.

The cell potential of 2.04 volts at an operating temperature of 70°C for the Stuart cell can be converted into a thermal efficiency rating with the aid of equations (20) and (21). First, using equation (21)

$$E_t = 1.505 \text{ v}$$

So that

$$\eta = \frac{1.505}{2.04} \times 100 = 74\%$$

The cell potential may also be compared to the thermodynamic reversible cell potential given by equation (17):

$$E_{\text{rev}} = 1.196 \text{ v}$$

calculated using an electrolyte concentration of 2S% KOH. The variation of cell potential with current density for the Stuart cell is shown in Fig. 1.

III D. TELEDYNE ISOTOPES

The Electra Cell manufactured by Teledyne is a bipolar filter press type using porous nickel electrodes and 25% KOH electrolyte at 180°F. Teledyne manufactures these in three sizes, the smallest being hydrogen generators producing between 10.6 and 21.2 cubic feet of hydrogen per hour. Their intermediate size systems produce between 10.6 and 4240 cubic feet of hydrogen per hour and their electrolysis plants produce 250 pounds or more of hydrogen per day with a nominal cell potential of 1.84 v and a current density of 400 amps per square foot (or 4300 amps per square meter). Since the current density can vary depending upon the particular use to be made of the electrolysis plant, Teledyne sizes their units using a computerized routine. The variation of required cell potential with current density for the Teledyne Electra Cell hydrogen plant is shown in Figure 1 along with a similar curve for an advanced cell which Teledyne expects to be commercial within the next three years.

The cell potential of 1.84 volts at 180°F corresponds to a thermal efficiency of

$$\eta = \frac{1.507}{1.84} \times 100 = 82\%$$

where the thermoneutral cell potential of 1.507 volts was calculated using equation (21). This may be compared with the thermodynamic reversible cell potential given by equation (17) with 25% KOH at 70 psig

$$E_{\text{rev}} = 1.223 \text{ volts}$$

Since Teledyne builds hydrogen plants to order for a specific application and optimizes these plants using a computer program, the current density of the plant will depend upon economic factors such as the cost of electricity and the utilization of the plant. As an example, the cost of a 25 ton per day hydrogen plant with a 100% utilization rate and a power cost of 10 mills per kilowatt-hour is optimized at \$6 million with current technology and \$4.5 million for the advanced cell. More expensive electricity would mandate more efficient operation (i.e., lower current density) which would tend to increase these figures. Electricity at 20 mills per kilowatt hour would increase these cost figures about twenty percent.

III E. LURGI APPARATE - TECHNIK, GMBH

Lurgi manufactures a high pressure Zdansky-Lonza cell which operates at 95°C and 30 atm̄ pressure with an electrolyte concentration of 25% KOH. With a current density of 1900 amps per square meter, the cell potential is 1.84 volts. The Zdansky-Lonza cell is of the bipolar filter press type and uses nickel-plated wire gauze electrodes. The variation of cell potential with current density for the Lurgi cell is shown in Figure 1. Lurgi is also developing a cell with a nominal current rating of 4000 amps per square meter in an effort to reduce capital costs. Lurgi estimates a cost reduction from 14.2 million dollars to 10.7 million dollars for a 25 ton per day hydrogen plant using the

higher current density. These costs include the electrolyzer, subsidiary units, and the electrical rectification equipment.

The thermal efficiency of the Lurgi high-pressure cell is

$$\eta = \frac{1.509}{1.84} \times 100 = 82\%$$

where once again the thermoneutral cell potential was calculated using equation (21). The thermodynamic reversible cell potential given by equation (17) with 25% KOH at 30 atm and 95°C is

$$E_{\text{rev}} = 1.252 \text{ volts}$$

III F. BAMAG VERFAHRENSTECHNIK GMBH

The electrolysis unit marketed by Bamag is a bipolar unit operating at 80°C with a current density of 2500 amps per square meter. The pressure is essentially atmospheric with an electrolyte concentration of 26% KOH. The cell potential for the Bamag cell at the nominal current density is 1.92 volts and the variation of this quantity with current density is shown in Fig. 1. Bamag estimates an electrolysis plant producing 7.6 tons per day of hydrogen to cost 2.67 million dollars.

The thermal efficiency of the Bamag electrolyzer is, with

a thermoneutral cell potential of 1.506 volts,

$$\eta = \frac{1.506}{1.92} \times 100 = 78\%$$

and the thermodynamic reversible cell potential is

$$E_{\text{rev}} = 1.186 \text{ volts}$$

Bamag is currently conducting research with the aim of producing larger, cheaper modules operating at a higher temperature.

III G. NORSK HYDRO VERKSTEDER A-S

This manufacturer supplies a bipolar filter-press electrolyzer which uses a 25% KOH solution at 80°C and a pressure of about 15 inches WG. With a nominal current density of 1500 amps per square meter, the cell potential is 1.87 volts. The variation of this quantity with current density is shown in Fig. 1.

The thermal efficiency of the Norsk Hydro electrolyzer is

$$\eta = \frac{1.506}{1.87} \times 100 = 81\%$$

and the thermodynamic reversible cell potential is

$$E_{\text{rev}} = 1.185 \text{ volts}$$

Norsk Hydro estimates the cost of a 95 ton per day hydrogen plant as \$39 million. No research is currently being conducted to improve efficiency or reduce costs.

III H. LIFE SYSTEMS, INC.

The static feedwater concept developed by Life Systems under NASA sponsorship was designed as part of a spacecraft waste reclamation system. According to Life Systems (ref. 17) this concept has terrestrial applications.

Basically, static feedwater electrolysis is carried out by transferring the water to the cell as a vapor produced as a result of a vapor pressure difference between the electrolyte solution and the feedwater. The electrolyte solution is supported in a matrix between catalyzed porous electrodes. The electrolyte is a 35% KOH solution, more concentrated than conventional cells so as to increase the vapor pressure difference which causes transfer of water from the feed compartment to the electrolyte. At present, the Life Systems cell is designed to withstand pressures up to 600 psi and temperatures up to 220°F at a current density of 600 amps per square foot (6460 amps per square meter) at a cell potential of 1.84 volts with projections into the near future of a cell operating at 2000 psi, 300°F with a current density of 1500 amps per square foot (16,200 amps per square meter) but an increased cell potential of 2.02 volts.

The thermal efficiency of the present technology Life Systems cell is

$$\eta = \frac{1.510}{1.84} \times 100 = 82\%$$

and the thermodynamic reversible cell potential is

$$E_{\text{rev}} = 1.261 \text{ volts}$$

The variation in cell potential with current density for the Life Systems cell is shown in Fig. 1.

III I. GENERAL ELECTRIC

In contrast to the previous cells, each of which uses a potassium hydroxide solution as the electrolyte, the electrolysis cell developed by GE uses a solid plastic sheet of perfluorinated sulfonic acid polymer as the electrolyte. This is coated on one side with a thin layer of platinum black to form the cathode and a similar thin layer of proprietary alloy catalyst is used for the anode. This system has been described in some recent papers by Titterington and others (ref. 18 and 19).

The advantages claimed for this system are, operation at high pressure (up to 3000 psi), and high current density (greater than 1000 amps per square foot), and the elimination of corrosive electrolyte which could carryover into downstream equipment. At a current density of 1000 amps per square foot (10800 amps per square meter) and a temperature of 180°F, the GE cell has a required cell potential of 1.85 volts. The thermal efficiency is then

$$\eta = \frac{1.506}{1.85} \times 100 = 81\%$$

and the thermodynamic reversible cell potential is

$$E_{\text{rev}} = 1.176 \text{ volts}$$

The variation of cell potential with current density for the GE solid polymer electrolyte cell at 180°F is shown in Fig. 1.

The capital cost of the GE solid polymer electrolyte cell is currently rather high due to the high cost of the solid polymer electrolyte itself as well as the previous metals used for the electrodes. GE is conducting research to lower these costs by developing a thinner electrolyte or an alternative solid to be used as the electrolyte. GE is also attempting to increase the cell efficiency through an increase in the operating temperature. The problem here is one of preventing cell degradation at the elevated

temperatures. By 1985, GE expects to increase cell operating temperature from the current 220°F up to 300°F.

Another factor to be considered in cost comparisons is the operating pressure. The GE electrolysis cell is capable of operating at pressures up to 3000 psi thereby eliminating the need for a compressor when hydrogen is required at pressures up to this value. On the other hand, this reduction in capital cost is not accompanied by a corresponding decrease in operating costs. Unlike all the other electrolysis cells, the GE unit shows no increase in efficiency as the pressure is increased. In fact, the cell voltage increases with rising pressure due to the power required for compressing the hydrogen.

III J. SUMMARY AND COMPARISON OF ELECTROLYSIS CELLS

The efficiency of the various electrolysis cells is shown in Fig. 1 in the form of a graph of the dependence of cell potential on current density. Typical design conditions and capital costs are summarized in Table 1. The capital costs represent only approximate figures. Accurate comparisons can only be made by establishing design criteria and requesting bids from manufacturers. Such items as degree of utilization, efficiency desired, and hydrogen pressure required will affect these costs.

The efficiency values shown in Fig. 1 and in Table 1 also deserve comment. As pointed out by Lurgi (ref. 11), the cell potential exhibits some fluctuation ($\pm 3\%$) and, according to Norsk Hydro (ref. 13), there is a net increase in this quantity with time of about 1 or 2% per year. Some of the manufacturers quote cell potential values after one year of operation, but this is not true for all and consequently, there is some degree of uncertainty present when making cell voltage comparisons.

IV MODELING OF ELECTROLYSIS CELL EFFICIENCY

The difference between the actual cell voltage and the reversible cell potential is due to three factors:

- a) chemical polarization at the electrodes,
- b) concentration polarization in the electrolyte; and
- c) ohmic losses in the electrolyte and across the membrane.

Each of these terms will be explored in some depth.

IV A. CHEMICAL POLARIZATION

Chemical polarization results from charge transfer inhibition at the electrode and is determined by the catalytic activity of the electrodes and the surface roughness. According to Eisenberg (ref. 4), chemical polarization can be represented as

$$\Delta E_{\text{chem}} = (RT / \alpha n F) \ln (\bar{\Phi} / \phi_c) \quad (22)$$

where α = transfer coefficient

ϕ_c = exchange current density

and $\bar{\Phi}$ = current density

The exchange current density is related to the height of the activation energy barrier, ΔF^*

$$\phi_c = kT \exp(-\Delta F^*/RT) \quad (23)$$

where k is a constant which incorporates Avogadro's number, the Boltzmann and Planck constants, the Faraday equivalent and the electrolyte concentration.

Equation (22) can be written in the more customary Tafel form

$$\Delta E_{\text{chem}} = a + b \ln \bar{\Phi} \quad (24)$$

in which the Tafel constants "a" and "b" depend on temperature.

According to equation (24), the variation in cell potential with temperature, $d(\Delta E_{\text{chem}})/dT$, is dependent upon electrolyte concentration and current density.

An electrolysis cell gives rise to two chemical polarization terms, one each at the anode and cathode. These are referred to as the oxygen and hydrogen overvoltage respectively:

$$\begin{aligned} \Delta E_{\text{O}_2} &= a_{\text{O}_2} + b_{\text{O}_2} \ln \bar{\Phi} \\ \Delta E_{\text{H}_2} &= a_{\text{H}_2} + b_{\text{H}_2} \ln \bar{\Phi} \end{aligned} \quad (25)$$

The values of the Tafel constants appearing in equation (25) have been reported by a number of investigators (ref. 20 to 23) with somewhat inconclusive results. The Tafel slope for hydrogen, b_{H_2} , is fairly well known at 25° C, and the constants for oxygen are greater than those for hydrogen. The influence of electrode material, electrolyte concentration and temperature on the Tafel constants is not very well known at this time although it is reported that commercial manufacturers have considerably more proprietary information than what has been reported in the literature.

Based on information available at the present time, the following values have been chosen as representative

$$\begin{aligned} \Delta E_{\text{O}_2} &= .6 + .055 \ln \bar{\Phi} \\ \Delta E_{\text{H}_2} &= .3 + .045 \ln \bar{\Phi} \end{aligned} \quad (26)$$

at 25°C for modern electrolysis cells with $\bar{\Phi}$ in amperes per square centimeter. The effect of temperature on cell performance has been reported (ref. 23) as follows:

$$O_2 - N_i = d (\Delta E)/dT = -.0033 \text{ V/}^\circ\text{C}$$

$$H_2 - Fe = d (\Delta E)/dT = -.0025 \text{ V/}^\circ\text{C}$$

at room temperature over a range of current density up to 2000 amperes per square meter.

Combining this data with equations (22), (23), (24) and (26), gives a total chemical polarization loss as

$$\Delta E_{\text{chem}} = 5.19 + 0.1 \ln \bar{\phi} - 0.8 \ln T \quad (27)$$

IV B. OHMIC LOSSES

The Ohmic loss in an electrolysis cell is the sum of the iR terms due to anolyte, membrane and catholyte resistances. The conductivity of KOH and NaOH solutions exhibit maxima when plotted versus concentration at constant temperature, and consequently, the electrolyte concentration is often chosen to be at this value so as to minimize the ohmic loss. For KOH solutions at 25°C, the maximum conductivity occurs at 20% KOH, increasing to 35% KOH at 80°C. In cell designs where the gases produced bubble up through (or with) the electrolyte, the bubbles contribute to the ohmic loss. In addition, vapor bubbles (H_2O) will also be produced further increasing the ohmic resistance. The volume rate of bubbles produced will depend upon pressure, temperature, electrolyte concentration and current density, and these factors together with electrolyte conductivity, membrane resistance and cell design considerations determine the ohmic loss in the electrolysis cell.

In order to determine the contributions of the above factors to the ohmic loss of an electrolysis cell, consider the model used by Funk and Thorpe (ref. 24):

The cell consists of electrodes of width W and height H separated by chambers for anolyte and catholyte flow with an internal membrane. Electrolyte enters the cell with an initial velocity V_{10} in the cathode chamber and velocity V_{20} in the anode chamber. By the stoichiometry of the electrolysis reaction, twice as much hydrogen as oxygen is produced on a molal basis. Assuming ideal gas behavior, this 2:1 ratio is true on a volume basis as well. If the bubble velocities for O_2 and H_2 are the same, and if $V_{10} = V_{20}$, placing the membrane such that $l_1 = 2l_2$ then gives the same gas-liquid ratio in both chambers. The bubble volume, however, also includes the volume of water vapor generated, but since the partial pressure of H_2O and the total gas pressure is the same on both sides of the membrane (assuming the gases are saturated with water vapor at the cell operating conditions), this 2:1 ratio is unaffected. Under the above assumptions, the resistivity of the electrolyte - gas mixture will be the same in both chambers.

The ohmic loss in the cell may now be written as

$$\Delta E_{\text{ohmic}} = \int R_c \quad (28)$$

where the effective cell resistance R_c is given by

$$R_c = \sum_{i=1}^2 r_f l_i f(\alpha_i) + R_m \quad (29)$$

where R_m = membrane resistance, ohm-cm²

= membrane resistivity (ohm-cm) * thickness (cm)

r_f = electrolyte resistivity (ohm-cm)

α = volume fraction of bubbles in the cell

$f(\alpha)$ = multiplier to obtain gas-liquid mixture resistance

Subscripts: 1 for catholyte chamber, 2 for anolyte chamber

Equation (29) contains, in addition to the aforementioned assumptions, the additional stipulation that the bubble boundary layer is formed quickly and fills up the entire chamber. Funk and Thorpe found this to be the case in their experimental investigation. Tobias (ref. 25) suggests calculating the resistance multiplier $f(\alpha)$ as

$$f(\alpha) = \frac{1}{\frac{1.5}{(1-\alpha)}} \quad (30)$$

whereas Mashovets' empirical equation (ref. 26) fits data in the range $0 < \alpha < .74$:

$$f(\alpha) = \frac{1}{1 - 1.78\alpha + \alpha^2} \quad (31)$$

The value of α will obviously vary in the direction of electrolyte flow, being zero at the cell inlet and increasing monotonically until the cell exit is reached. The value of α at the cell exit may be

calculated by noting that the rate at which gas leaves the cell is equal to the rate at which it is generated. Consequently,

$$\alpha_e = \frac{A\bar{z}}{nF} \frac{RT}{P} \left(\frac{A\bar{z}}{nF} \frac{RT}{P} + \sigma V_0 W \bar{z} \right)$$

where α_e is the volume fraction of bubbles in the electrolyte leaving the cell, and σ is the slip ratio, defined as (gas velocity/liquid velocity). The value α_e must be corrected in order to include the vapor in the bubbles.

Assuming that the gas is saturated with vapor and letting p_s^0 represent the vapor pressure of the solution at the cell operating temperature, the modified equation for the volume fraction of bubbles in the exiting electrolyte becomes

$$\alpha_e = \frac{A\bar{z}RT}{A\bar{z}RT + nF(P-p_s^0)\sigma V_0 W \bar{z}} \quad (32)$$

Equation (32) holds for both the anolyte and catholyte chambers, and in fact, with the previously stated assumptions, yields the same value for each if the slip ratio is the same in each chamber. This is easily seen since $n = 2$ for the cathode chamber and $n = 4$ for the anolyte chamber and $l_1 = 2 l_2$, all other values being the same in the two chambers. In terms of volumetric electrolyte flow rate per unit area of electrode surface, $v = l W V_0/A$, equation (32) becomes

$$\alpha_e = \frac{1}{1 + nF \frac{(P-p_s^0)}{RT\bar{z}} \sigma v} \quad (33)$$

The value of the void fraction to be placed into equation (31) must be some average over the electrode surface. For this one-dimensional problem, a simple arithmetic average gives

$$\alpha = (1/2) \alpha_e \quad (34)$$

A better average is not easily obtained. The problem is that the current density varies in the flow direction, not the voltage. The bubble generation rate is, therefore, not uniform over the surface and the makeup of the voltage across the cell will vary with position. At the bottom (electrolyte inlet to the cell) the bubble resistance is low. As bubbles are formed, the ohmic loss increases and the current density decreases, thereby also affecting the chemical polarization contribution.

The resistivity of the electrolyte solution, r_f , is obtained from equivalent conductivity (Λ) data as

$$r_f = \frac{1000}{N\Lambda}$$

in which N is the normality of the solution. The quantity Λ is a function of N as well as temperature. Data from Perry (ref. 27) at 18°C are corrected for temperature variations using

$$r_f = \frac{r_{f \text{ } 18^\circ\text{C}}}{1 + m(t - 18)} \quad (36)$$

where t = temperature, °C

m = temperature coefficient, .02 - .025 for bases.

Kirk and Othmer (ref. 28) suggest a value of .022 for m except for strong bases (such as KOH), but this value correlates well the data for 28% KOH (ref. 29).

The final term in equation (29), the ohmic resistance of the membrane, depends on the membrane construction. Modern electrolysis cells use

an asbestos membrane which may be similar to the fuel cell asbestos studied by TRW (ref. 30) for which they report values as follows:

$$\begin{aligned} R_m &= .24 \text{ ohm-cm}^2 \text{ for 20 mil thickness} \\ &= .36 \text{ ohm-cm}^2 \text{ for 60 mil thickness} \end{aligned}$$

D. Soltis (of Lewis) reports a value of $.20 \text{ ohm-cm}^2$ for 10 mil asbestos in 14N KOH.

∴ In summary, the ohmic loss in a water electrolysis cell may be calculated if the following quantities are known: the electrolyte concentration, pressure, temperature, electrolyte flow rate per unit electrode area, cell width, gas bubble slip ratio in the anolyte and catholyte chambers, current density and membrane resistance. The temperature and electrolyte concentration together determine the vapor pressure of the solution which has been correlated (ref. 31) for temperatures less than 25°C as

$$\frac{p_s^o}{p_w^o} = 1 - .055N \quad (37)$$

where p_s^o = vapor pressure of the electrolyte solution, and

p_w^o = vapor pressure of water at the same temperature.

Data at higher temperatures (ref. 32) are also well correlated by this expression. Vapor pressure data for water may be obtained from standard sources.

IV C CONCENTRATION POLARIZATION

Concentration polarization results from concentration gradients

which exist in the neighborhood of the electrode and is small for a cell with circulating electrolyte. This contribution to the cell voltage is usually either ignored or lumped with the chemical polarization terms. Since this term arises due to a resistance to mass transfer, anything that tends to reduce mass transfer resistance will reduce the effect of this term. Thus, concentration polarization may be reduced in any of the following ways:

- 1) increasing the temperature
- 2) increasing the electrolyte flow rate
- 3) increasing the concentration of the species being transported; i.e., use greater strength KOH solutions
- 4) decreasing the spacing between electrodes
- 5) decreasing the current density

No data have been found in this area. Eisenberg (ref. 22) states that

$$\Delta E_{\text{conc}} = \frac{RT}{nF} \ln \frac{\bar{\Phi}_l}{\bar{\Phi}_l - \bar{\Phi}} \quad (38)$$

where $\bar{\Phi}_l$ is the limiting current density, a complex function of solution properties and hydrodynamic factors. For fully developed Poiseuille flow, Linton and Sherwood (ref. 33) give

$$\bar{\Phi}_l = 1.61 n F C_o \left(\frac{D}{l}\right)^{2/3} \left(\frac{V_o l}{H}\right)^{1/3} \quad \text{amp/cm}^2 \quad (39)$$

where C_o = ionic concentration, g moles/cm³

V_o = electrolyte velocity, cm/sec

l = thickness of electrolyte, cm

D = diffusion coefficient, cm²/sec

H = electrode length, cm.

The diffusion coefficient is given by Ibl (ref. 34) as

$$D = \frac{RT\lambda}{nF^2} \quad (40)$$

where λ is the equivalent conductivity of the solution.

The temperature dependence of λ can be obtained by combining equations (35) and (36). Equations (38) through (40) may now be combined to estimate the concentration polarization. Note that $V_0 l / H$ in equation (39) is the electrolyte flow rate per unit electrode area, W in equation (33).

The above calculations do not account for the presence of gas bubbles which hinder the diffusion of chemical species. This hindrance may be estimated by assuming that the active electrode area is reduced in proportion to the bubble fraction. The net result of this argument is to introduce a factor $(1 - \alpha)$ into the right hand portion of eq. (39).

IV D CELL VOLTAGE SUMMARY

The actual cell voltage may now be evaluated as

$$E = E_{\text{rev}} + \Delta E_{\text{chem}} + \Delta E_{\text{conc}} + \Delta E_{\text{ohmic}} \quad (41)$$

The reversible cell potential, E_{rev} , is given by eq. (17); the chemical polarization term, ΔE_{chem} , is shown in eq. (27). Ohmic loss is obtained by a complex analysis leading eventually to eq. (28); concentration polarization is given by eq. (38).

The effects of operating variables and cell design on the actual cell voltage may now be stated in a qualitative way. Operating

temperature affects all the terms in eq. (41). An increase in temperature decreases all but the last term in eq. (41). The ohmic loss depends on temperature through the void fraction α and the resistivity r_f . The negative effect of increasing void fraction due to increased temperature can be offset by operating at higher pressure and, possibly, with a higher strength KOH electrolyte solution to minimize vaporization. In any event, it would appear that operation at the maximum allowable temperature is desirable. Of course, there are also energy losses associated with cooling the gaseous products but the magnitude of these losses may be minimized by suitable heat recovery systems.

As mentioned above, increasing the pressure has at least one positive impact for electrolysis cells; that is, it reduces the volume of the gas bubbles produced and also reduces vaporization of the solution which adds to the total gas flow for the system. There is, however, a beneficial aspect of vaporizing the water in solution. Namely, this vaporization process tends to maintain the cell operating temperature without the use of high electrolyte circulation rates which can result in the need for an appreciable amount of pumping power. In addition to the above, increasing the pressure increases the reversible cell potential and has an unknown effect on the chemical polarization and concentration polarization terms.

The main effect of changing the concentration of the KOH electrolyte is on the ohmic loss in the cell. The resistivity of the solution passes through a minimum as KOH concentration is increased thereby suggesting a concentration level for cell operation, although the effect of KOH concentration on the concentration polarization has prompted consideration of the use of somewhat higher concentrations than those indicated by conductivity arguments (ref. 35). In addition

to these effects, there is the aforementioned effect of KOH concentration on vaporization of water from the electrolyte solution and the increase in E_{rev} associated with increasing KOH concentration as dictated by thermodynamics and the Nernst equation.

An increase in current density will not affect E_{rev} but will increase each of the loss terms shown in eq. (41). The tradeoff between operating efficiency and capital cost that results from this has already been discussed.

Electrolyte velocity plays a role in the determination of the ohmic resistance of the cell and also the concentration polarization. Increasing the velocity reduces the void fraction due to bubbles, helps to maintain a more uniform temperature profile and increases the limiting current of the cell; consequently, both ΔE_{conc} and ΔE_{ohmic} are reduced. Selection of the optimum velocity is then a tradeoff between the above cell efficiency considerations and the power required for electrolyte circulation.

Electrode design is a very important factor in the performance of a water electrolysis cell. Such items as construction material, surface preparation, electrode spacing and cell dimensions play a major role in the determination of polarization and ohmic losses in the cell. Electrode material significantly influences the Tafel constants for chemical polarization, particularly the "a" values. The choice of nickel and nickel-plated steel for the anode is made based on consideration of these Tafel constants vs. availability and cost. Exotic materials such as platinum can reduce these losses somewhat but not economically for large scale usage. For special situations, other factors could make the use of these materials desirable.

Treating the electrode surface so as to provide a greater effective area also reduces chemical polarization losses. This can be done by using porous electrodes (ref. 11), "dimpling" or activating the electrode surface (ref. 13) or by employing finned electrodes (ref. 16) or electrode strips (ref. 36). In any event, the increased area acts to reduce the effective current density at the surface, thereby reducing the chemical polarization loss as given by the Tafel equation.

The effects of electrode spacing and cell size come directly from the equations presented in the previous sections. Equations (38) and (39) indicate that concentration polarization decreases as the electrode size increases and the spacing between electrodes decreases. Starting with widely spaced electrodes, decreasing the spacing at first reduces ohmic losses due to the shorter distance as seen in equation (29). At some point, however, as the electrodes become closer, the effect of the gas bubbles becomes important and eventually dominates, causing an increase in the ohmic loss. These effects are shown in equations (30) and (32). There is then an optimum electrode spacing which will result in a minimum cell voltage. This optimum spacing may turn out to be less than can be effected by modern construction techniques (ref. 1).

As indicated in the previous sections, rapid recirculation of the electrolyte will reduce both ohmic and concentration polarization losses. The ohmic resistance is decreased due to the sweeping away of the gas bubbles. This same sweeping effect also reduces the concentration gradients formed. The savings in cell voltage must be balanced against the increased pumping power requirement in an overall efficiency optimization.

Some of the methods for improving cell efficiency discussed above will result in increased capital cost requirements necessitating the establishment of tradeoffs between the two. One obvious area in which this occurs is in the selection of an operating pressure. A higher pressure generally results in increased cell efficiency, but requires heavier and, hence, more costly construction, not only of the electrolysis module, but for much of the auxiliary equipment as well. There is also the safety aspect of handling hot lye under pressure which may dictate the use of more costly control systems. For these reasons, an economic study should consider the entire electrolysis plant. Similar arguments can lead eventually to the adoption of a systems study program which integrates the electrolysis plant into the environment of its use. Minimum cost of hydrogen produced may not be desirable, for example, when the hydrogen is being used as an energy storage medium for a large electrical power generating facility. In such cases, electrolysis cell efficiency may be an overriding factor in producing electricity at the lowest possible price. Such considerations, however, are beyond the scope of this report.

In summary, equations in the preceding sections allow the calculation of electrolysis cell voltage, which is inversely proportional to the cell efficiency, when the following quantities are known:

Operating temperature

Cell pressure

Current density

Electrolyte (KOH) concentration

Tafel constants, oxygen and hydrogen sides

Electrode-to-membrane spacings

Membrane resistance

Electrode size (height or diameter)

Electrolyte flow rate per unit area of electrode

From the above list, several quantities may be optimized, whereas selection of some others is governed by considerations not related to cell efficiency. The choice of an operating temperature, for example, cannot be made based on cell voltage since the latter is a monotonic function of temperature. Operation at the highest temperature which still allows the maintenance of cell integrity is then indicated. There are, of course, tradeoffs in all considerations, and cell efficiency is just one consideration in electrolysis cell design.

IV. E. Model Verification

The algorithm presented in the preceding sections has been assembled as a computer simulation model for electrolysis cell potential. This model was tested against both commercial and research cell data. Figure 3 shows the variation in cell potential with current density for three manufacturers, along with predictions obtained using the model. Although there are differences in slopes and intercepts between the commercial data and the model predictions, the model does show clearly the superiority of the Teledyne design.

The model also correctly indicates the effects of pressure and temperature on electrolysis cell potential as reported by investigators at Oklahoma State University (ref. 37). The values shown in Figures 4 and 5 are in rather good agreement with the OSU data except at low temperatures.

The differences between the data and the values predicted using the computer simulation model shown in Figures 3, 4 and 5 is most probably largely due to the lack of information concerning electrolyte flow rate. The cell potential is rather sensitive to variations in this parameter whose value is not reported by either commercial manufacturers or academic researchers. In order to apply the simulation model, a simple equation was developed based on some of the cell potential data reported by investigators at Oklahoma State University:

$$V = .07 (4 - .003T) \left(.003 + \frac{1}{P} \right) \phi^{1.6} \quad (42)$$

in which V is the electrolyte flow rate per unit electrode area, whose value is required in equation (33). Since the simulation model uses this empirical relation, it can be expected to give the greatest agreement with data from which the equation was assembled. This is indeed the case. The best agreement occurs for the high temperature OSU data which was used to obtain equation (42). It is to be noted, however, that the agreement with commercial cell data shown in Figure 3 is rather good when one considers that equation (42) was used in obtaining the model predictions and this equation was developed independent of the commercial cell data.

The simulation model was used to describe the effects of variations in pressure, temperature, current density and electrolyte concentration on the cell potential and its various components. For this purpose, a base case was selected and variations about this base case were examined. The base case operating parameters chosen were as follows:

temperature:	375° K
pressure:	30 atm
current density:	0.6 amps/cm ²
electrolyte:	6 N KOH

The effect of pressure on cell potential is shown in Figure 6. As the pressure is increased, the reversible cell potential increases due to the work of compression of the generated gases. On the other hand, the ohmic resistance drops due to a reduction in the volume of these gases. For the design shown in Figure 6, this results in a decrease in the electrolysis cell potential over the range shown, although in principle, an optimum pressure will be attained beyond which the increase in the reversible cell potential overshadows the reduction in the ohmic loss.

The corresponding picture for current density is shown in Figure 7. For low current densities, the major cause of inefficiency is seen to be due to chemical polarization at the electrodes. As the current density is increased, the ohmic loss becomes increasingly important.

The effect of temperature on cell performance is shown in Figure 8. Initially, increasing the temperature results in a decrease in cell potential due mainly to a reduction in chemical polarization. Eventually, a point is reached where the ohmic loss begins to increase. This is due to vaporization of the electrolyte solution itself as shown by the sharp increase noticed as the boiling point of the solution is approached.

Figure 9 shows the effect of electrolyte concentration on the ohmic resistance of the solution. The minimum cell potential occurs almost exactly at the point of maximum conductivity.

V. Electrolysis Cell Dynamics

Electrolyzers have been suggested for the storage of energy derived from either off-peak power, wind or solar energy through conversion into hydrogen. In such applications, the voltage supplied to the electrolyzer can be expected to vary over a rather wide range. Depending upon the

time scale of the voltage variations, the electrolyzer dynamics may be important, and in fact a favorable dynamic situation could be exploited through the use of an intentionally-varying voltage input. This has led to suggestion of a pulsed mode of operation for electrolyzers.

It is not clear that intentional cyclic operation (e.g., pulsed operation) will improve the operating characteristics of an electrolyzer. Alternate periods in which voltage is applied and removed may in fact have a detrimental effect on the system in that it may cause control problems for the gas removal system. The possibility of causing a decrease in gas purity also exists. For these reasons, Norsk (ref. 13) advises maintaining a base load equal to 25% of rated capacity at all times and going above this up to rated capacity or more when power is available.

In pulsed electrolysis (i.e., on-off operation), bubbles of gas produced during the "on" period have the opportunity to leave the system during the "off" portion of the cycle. The benefit achieved through the use of this pulsed electrical input lies then in the reduced resistance, and consequently increased efficiency, during the "on" period as a result of the reduction in bubble volume. As a limiting case, the electrolysis cell model described earlier can be executed assuming zero bubble volume. This would give the best improvement in performance that could be expected. The net reduction in cell potential is shown parametrically in Figure 10 for a particular cell design with operating parameters as listed. If the current density for the pulsed cell is the same as that for the normally operating cell, a reduction in cell potential of .2-.3 volts can be achieved. This is a sizeable reduction but the comparison can be somewhat misleading. If the pulsed unit is the same size as the normally operating unit, then the pulsed cell will produce less hydrogen because it only operates during a part of the cycle.

The two modes of operation may also be compared under conditions of equal hydrogen production rate. Since the pulsed electrolyzer only operates for a fraction of the time, it must operate at a higher current density during that time in order to compensate for the remaining time. Let B represent the fraction of the cycle for pulsed operation during which the electrolyzer is operating. Then if ϕ_1 is the current density for normal operation and ϕ_2 the current density for the pulsed mode, equal hydrogen production rates are obtained when

$$B \phi_2 = \phi_1$$

or

(43)

$$\phi_2 = \frac{\phi_1}{B}$$

The higher current density during pulsed operation will result in a decrease in cell efficiency. When this effect is combined with the improvement in efficiency as a result of removal of the gas bubbles, it is not clear whether or not pulsed operation is desirable.

Suppose that the pulsed electrolyzer operates with equal time intervals for "on" and "off" so that $B = 1/2$. Then equation (43) indicates that $\phi_2 = 2 \phi_1$. Defining voltage reduction once again as E pulsed - E normal, gives the voltage reduction curve labeled "equal hydrogen production rates" in Figure 10. In this case, the abscissa is ϕ_1 , the current density for the normally-operating cell and the value of ϕ_1 influences the choice between pulsed mode or normal operation. For the particular case shown, pulsed operation is desirable if ϕ_1 is less than 0.5 amps/cm² but is undesirable if ϕ_1 is greater than 0.5.

The dynamics of electrolysis cells should not be dismissed based on the preceding analysis. That is, the electrical energy source for

an electrolyzer may be generated by a varying power source such as photovoltaic or wind energy. Under such circumstances, the electrolyzer may be operated directly with this varying input, or it may be operated at a constant input through the use of a conventional power source when needed to supplement the primary energy input. Figure 10 indicates that this choice is controlled by electrolysis cell dynamics together with the dynamics of the energy source.

VI Summary and Conclusions

The analysis presented in this paper has led to a simple mathematical description of electrolyzer performance. This model is not claimed to be universally applicable and accurate - there are too many assumptions and unknown parameters for that to be true. However, the model does give a good representation of the effects of pressure, temperature and current density as is seen in Figures 3, 4 and 5, and this in turn endows the model with at least some credibility. As a next step, the model could be integrated into a multiparameter, optimization routine which would find the best designs and operating conditions subject to constraints such as temperature and pressure maxima.

More importantly, the model indicates the relative magnitudes of each of the losses involved in electrolysis cell operation. For example, it was found that concentration polarization effects were negligible and for this reason, this term does not appear in Figures 6, 7, 8 and 9. In addition, the model helps to create a better understanding of these losses, and is used to predict the possible advantage of operating an electrolysis cell with a pulsed electrical input.

Based on the present study, it appears that further research is needed to establish a more thorough understanding of the overvoltages in an electrolysis cell. This research should combine theoretical aspects with experimental information. At the same time, research into

novel approaches to electrolyzer design and/or operation should be encouraged. Such research might include use of a pulsed electrical input or use of sunlight to reduce the voltage requirement of the cell through activation of the electrodes. Finally, a better understanding of cell dynamics is required in order to assess the feasibility of coupling an electrolysis cell to an unsteady power source.

REFERENCES

1. Costa, R. L.; and Grimes, P. G.: Electrolysis as a Source of Hydrogen and Oxygen. Chem. Eng. Prog. Symp. Ser., vol. 63, no. 71, 1967, pp. 45-58.
2. Mantell, Charles. L.: Hydrogen, Oxygen, and Deuterium, Electro-Chemical Engineering, Ch. 12, 4th ed., McGraw-Hill Book Co. Inc., 1960, pp. 308-319.
3. Schade, C. W.; et al.: Energy Depot Electrolysis Systems Study. TID-20441-Vol.-1, Atomic Energy Commission, 1964.
4. Design Study of Hydrogen Production by Electrolysis, Volume 1. ACSDS-0106643, Allis-Chalmers Mfg. Co. (TID-23439), 1966.
5. Chapman, E. A.: Production of Hydrogen by Electrolysis. Chem. Proc. Eng., vol. 46, no. 8, Aug. 1965, pp. 387-393.
6. Stuart, A. K.: Modern Electrolyser Technology in Industry. Presented at Am. Chem. Soc. Ann. Nat'l Meeting, Symposium on Non-Fossil Chemical Fuels, Boston, April 1972.
7. Gregory, D. P.: A Hydrogen-Energy System. Rept. L211/3, Am. Gas Assoc., 1972.
8. McAlevy, R. F. III, et al.: Hydrogen As a Fuel. ME-RT-74011, Stevens Inst. Tech. (AD-787484), 1974.

9. Kippenhan, C.; and Corlett, R. C.: Exploratory Engineering Research in Energy Management and Utilization. Seattle City Light Contract from Dept. Mech. Engr., Univ. Washington, 1973.
10. Wydeven, T.; and Johnson, R. W.: Water Electrolysis: Prospect for the Future. J. Eng. Ind., ASME Trans., vol. 90, Nov. 1968, pp. 531-540.
11. Lurgi Apparate - Technik GMBH, Frankfurt, Germany: Electrolysis units production specification.
12. Teledyne Isotopes, Timonium, Md.: Electrolysis units production specification.
13. Norsk Hydro a.s., Oslo, Norway: Electrolysis units production specification.
14. Bamag Verfahrenstechnik GMBH, Butzbach, Germany: Electrolysis units production specification.
15. The Electrolyser Corporation Ltd., Toronto, Ont.: Electrolysis units production specification.
16. Allison, H. F.; Ramukar, R.; and Hughes, W. L.: Economic High-Pressure Hydrogen-Oxygen Regenerative Fuel-Cell Systems. Proc. 4th Intersoc. Energy Conversion Engineering Conf. Am. Inst. Chem Engrs., 1969, pp. 1042-1047.
17. Jensen, F. C.; and Schubert, F. H.; Hydrogen Generation Through Static-Feed Water Electrolysis. Proc. the Hydrogen Economy Miami Energy Conf., Plenum Press, 1975, pp. 425-439.

18. Spacil, H. S.; and Tedmon, C. S., Jr.: Electrochemical Dissociation of Water Vapor in Solid Oxide Electrolyte Cells.
- I - Thermodynamics and Cell Characteristics. J. Electrochem. Soc., vol. 116, no. 12, Dec. 1969, pp. 1618-1626.
- II - Materials, Fabrication, and Properties. J. Electrochem. Soc., vol. 116, no. 12, Dec. 1969, pp. 1627-1633.
19. Nuttall, L. J.; Fickett, A. P.; and Titterington, W. A.; Hydrogen Generation by Solid-Polymer Electrolyte Water Electrolysis. Proc. Hydrogen Economy Miami Energy Conference, Plenum Press, 1975, pp. 441-455.
20. Lange's Handbook of Chemistry. 11th ed., McGraw Hill 1973.
21. Hampel, Clifford A., ed.: The Encyclopedia of Electrochemistry. Reinhold Publishing Corp., 1964, pp. 1795-96.
22. Eisenberg, M.: Design and Scale-up Considerations for Electrochemical Fuel Cells. Advan. Electrochem. Electrochem. Eng., vol. 2, 1962, pp. 235-291.
23. Bowen, C. E.: Production of Hydrogen and Oxygen by the Electrolysis of Water. J. Inst. Elec. Engrs. (London), vol. 90, pt. 1, 1943, pp. 478-485.
24. Funk, J. E.; and Thorp, J. F.: Void Fraction and Current Density Distributions in a Water Electrolysis Cell. J. Electrochem Soc., vol. 116, no. 1, Jan. 1969, pp. 48-54.
25. Tobias, Charles W.: Effect of Gas Evolution on Current Distribution and Ohmic Resistance in Electrolyzers. J. Electrochem. Soc., vol. 106, no. 9, Sept. 1959, pp. 833-839.
26. Mashovets, V. P.: The Effect of Nonconducting Inclusions on the Conductance of an Electrolyte. J. Appl. Chem., USSR, vol. 24, 1951, pp. 391-398.

27. Perry, John H., ed.: Chemical Engineers' Handbook. 3rd ed., 1950, p. 1782.
28. Kirk, Raymond E.; and Othmer, Donald F.: Encyclopedia of Chemical Technology. Vol. 7, Interscience Publ., 1965, p. 825.
29. Clifford, J.; Research on the Electrolysis of Water under Weightless Conditions. MRL-TDR-62-44, Battelle Memorial Inst., 1962.
30. Vogt, J. W.; Materials for Electrochemical Cell Separators. (TRW-ER-7055-4; TRW Equipment Labs.; NAS3-8522), NASA CR-72493, 1968.
31. Bro, P.; and Kang, H. Y.: The Low-Temperature Activity of Water in Concentrated KOH Solution. J. Electrochem. Soc., vol. 118, no. 9, Sept. 1971, pp. 1430-1434.
32. Dyson, W. H.; et al.: Physical-Chemical Studies of KOH-ZnO Electrolyte. J. Electrochem. Soc., vol. 115, no. 6, June 1968, pp. 566-569.
33. Linton, W. H., Jr.; and Sherwood, T. K.: Mass Transfer From Solid Shapes to Water in Streamline and Turbulent Flow. Chem. Eng. Prog., vol. 46, 1950, pp. 258-264.
34. Ibl, N.: Applications of Mass Transfer Theory: The Formation of Powdered Metal Deposits. Advan Electrochem. Electrochem Eng., vol. 2, 1962, pp. 49-143.
35. Rhodes, W. A.: Electrolytic Production of Hydrogen and Oxygen. U.S. Patent 3,394,062, July 23, 1968.
36. Silman, H.: Electrolytic Hydrogen - Its Manufacture and Applications. Chem. Age, vol. 93 Jan. 16, 1965, pp. 126-127.
37. McCollom, Kenneth A.: Use of Energy Storage with Unconventional Energy Sources to Aid Developing Countries. Advances in Energy Conversion Engineering, Am. Soc. Mech. Engrs., 1967, pp. 813-819.

APPENDIX

The Computer Simulation Model

This program calculates the cell potential for an electrolysis cell of a given design with stated operating parameters. The design variables and operating parameters are the following:

pressure = P, atm

temperature = T, °K

current density = PHI, amps/cm²

electrolyte (KOH) concentration = CONC, weight fraction, weight percent or normality

slip ratio = SRA, SRC - ratio of bubble velocity to electrolyte velocity for anode and cathode chambers respectively

flow rate ratio = WR, ratio of electrolyte flow rate in cathode chamber to that in anode chamber

cell width ratio = LR, ratio of width of cathode chamber to that of anode chamber

electrolyte flow rate = W, cc's per second per square centimeter of electrode area

cell width = L, cm

cell height = H, cm

membrane resistance = RM, ohm-cm², = membrane resistivity (ohm-cm) *thickness (cm)

Since in a given analysis some of these parameters may be unknown, the program uses Namelist input with a default option. In this type of input, the variables are assigned to a Namelist. For this program, the assignments are as follows:

Namelist/OPVAR/PHI, P, T, CONC
Namelist/RATIO/SRA, SRC, WR, LR
Namelist/CELL/W, L, H, RM

The data stack is composed of $3n+1$ cards in which n is the number of sets of data to be run as specified on the first data card using an I2 format. For each data set, there is one data card for each Namelist parameter list. These cards are typed with a "\$" in column two followed immediately by the Namelist Name (OPVAR, CELL, or RATIO). The data is then listed in equation assignment form (e.g., $p = 5$, $T = 400$) with separating commas. Not all of the data need be specified. Those items not specified will remain at the values used in the previous data set. For the first data set, the default values are as follows:

P = 1, T = 350, CONC = 6, PHI = 0.2
SRA = SRC = 1, WR = LR = 2
L = 0.3, H = 100, RM = 0.1

If W is not included in the specification of the first data set, it is calculated using equation (42) ($V = W$). If it is desired to use this equation for subsequent data sets, a negative value must be assigned to W in the CELL Namelist. The program listing followed by a sample data set and the corresponding output completes this Appendix.

PROGRAM LISTING

Main Program

```
COMMON /AA/ A(12)
COMMON /BB/ B(6)
COMMON /CC/ C(8)
READ (5,11) N
DO 10 I=1,N
CALL TMTT
CALL PTNTL
CALL PRNTR
GOTO CONTINUE
GOTO 11 FORMAT (I2)
STOP
END
```

First Subroutine - Default Option

```
BLOCK DATA
COMMON /AA/ P,T,CONC,PHI, RAO(4),W,L,H,PM
REAL L
DATA P,T,CONC,PHI,(RAO(I),I=1,4),,L,H,PM/1.,350.,6.,0.2,1.,1.,
1 2.,2.,-1.,0.3,100.,0.10 /
END
```

```

SUBROUTINE INIT
COMMON /AA/ P,T,CONC,PHI,SRA,SRC,WR,LR,W,L,H,RM
COMMON /BB/ WA,WC,L1,L2,X,N
REAL LR,L,L1,L2,X,N
NAMCLTST /OPVAR/ PHI,P,T,CONC
NAMCLIST /RATIO/ SRA,SRC,WR,LR
NAMCLTST /CELL/ W,L,H,RM
WRITE (5,181)
READ (5,OPVAR)
WRITE (5,OPVAR)
IF (CONC .LT. 0. .OR. CONC .GT. 100.) GO TO 130
IF (CONC .GT. 1.) GO TO 115
X = CONC
00110 N = 10.*X*(X+1.)
GO TO 135
00115 IF (CONC .GE. 15.) GO TO 125
N = CONC
00120 X = -0.5 + SQRT(0.25+(N/10.))
GO TO 135
00125 X = 0.01*CONC

GO TO 110
00130 WRITE (5,180)
N = 5.
GO TO 120
00135 READ (5,RATIO)
WRITE (5,RATIO)
READ (5,CELL)
WRITE (5,CELL)
WA = W/(WR+1.)
WC = WA*WR
L2 = L/(LR+1.)
L1 = L2*LR
00180 FORMAT (44H ILLEGAL VALUE FOR CONCENTRATION, ON ASSUMED )
00181 FORMAT (141)
RETURN
END

```


Subroutine to Calculate Cell Potential

```

SUBROUTINE PTNTL
COMMON /AA/ P,T,CONC,PHI,SRA,SRC,WR,LR,W,L,H,RM
COMMON /BB/ WA,WC,L1,L2,X,N
COMMON /CC/ E,EREV,DECHM,DECHM(4),DECON
REAL L,L1,L2,LR,N,LAM,LAMIN

C
C THIS SUBROUTINE EVALUATES THE CELL POTENTIAL
C FOR THE DESIGN SPECIFIED
C
C THE REVERSIBLE CELL POTENTIAL - NERNST EQUATION
00200 CREV = 1.449 + 10.646*ALOG(P)+2.7*X**2+1.977-1.625*ALOG(T)*T*10.
1*(-4)

C
C CHEMICAL POLARIZATION VIA THE TAFEL EQUATION
C MODIFIED FOR TEMPERATURE VARIATION
DECHM = 5.19 + 0.1*ALOG(PHI) - 0.8*ALOG(T)
IF (DECHM .LT. 0.) DECHM=0.

C
C VAPOR PRESSURE CORRELATIONS
PWC=10.***(7.117 - (222./T))
PSC = PWC*(1.-0.055*N)/14.7
IF (PSC .LT. P) GO TO 215
WRITE (6,284) PSC
P = 1.2*PSC
00215 IF (W .GT. 0.) GO TO 220
W = 0.07*(4.-0.007*T)+(0.003+(1./P))*(PHI**1.6)
WA = W/(WR+1.)
WC = WA*WR

C
C BUBBLE VOLUME CALCULATION
00220 QC = 2352.*SRC*WC*(P-PSC)/(T*PHI)
QA = 2.*QC*SRA/(SRC*WR)
ALPHC = 1./(QC+1.)
ALPHN = 1./(QA+1.)

C
C RESISTANCE MULTIPLIER CORRELATION
FC = 1./(1.-ALPHC)**1.5
FC = (1.+2.*FC)/3.
FA = 1./(1.-ALPHN)**1.5
FA = (1.+2.*FA)/3.

C
C CORRELATION FOR EQUIVALENT CONDUCTIVITY
00230 LAM = 225.*10.**(-N/15.)

C
C RESISTIVITY OF KOH WITH TEMPERATURE CORRECTION
RFA = 1000./(N*LAM)
RF = RFA/(1.+0.022*(T-291.))

```

REPRODUCIBILITY OF THE
ORIGINAL PAGE IS POOR

Cell Potential Calculation - Continued

```

C      OHMIC LOSS CALCULATIONS
      DEOHM(4) = PHI*RM
      DEOHM(2) = L2*FA*RF*PHI
      DEOHM(3) = L1*FC*RF*PHI
      DEOHM(1) = DEOHM(2) + DEOHM(3) + DEOHM(4)
C
C      EQUIVALENT CONDUCTIVITY
      AND DIFFUSION COEFFICIENT CALCULATIONS
00240 LAMIN = 1000./(N*RF)
      D = 7.953*10.**(-10)*T*LAMIN
C
C      LIMITING CURRENT DENSITY CORRELATIONS
      PHILIM = 321.4*N*MA**(1./3.)*(D/L2)**(2./3.)
C
C      CHECK ON ASSIGNED CURRENT DENSITY
      IF (PHI .LT. PHILIM) GO TO 250
      WRITE (6,290) PHI,PHILIM
      DECON = 0.
      GO TO 290
C
C      CONCENTRATION POLARIZATION
00250 Q = 2.15*10.**(-5)*T
      DECON = Q*ALOG(PHILIM/(PHILIM-PHI))
C
C      CELL POTENTIAL
00290 E = 5REV + DEOHM + DEOHM(1) + DECON
C
00280 FORMAT (42H ***** CURRENT DENSITY EXCEEDS LIMIT ***** ,
      1/ 5H PHI = ,F10.4 / 5H PHILIM = , F10.4)
00284 FORMAT (79HGTHE VAPOR PRESSURE OF THE ELECTROLYTE EXCEEDS THE ASSI
      GNED OPERATING PRESSURE / 44H PRESSURE REASSIGNED AS 1.20*PSO WHE
      2RE PSO = , F10.4, 4H ATM )
      RETURN
      END

```

Subroutine to Print Out Results

REPRODUCIBILITY OF THE ORIGINAL PAGE IS POOR

```

SUBROUTINE PRNTR
COMMON /AA/ P,T,CONC,PHI,SRA,SRC,WR,LR,W,L,H,PM
COMMON /BB/ WA,WC,L1,L2,X,N
COMMON /CC/ E,EREV,DECHM,DECHM(4),DECON
REAL LR,L,L1,L2,X,N

C
C PRINT OUT DESIGN SPECIFICATIONS
00305 WRITE (6,401)
WRITE (6,402) P,T,PHI,N

C
C PRINT OUT CELL DATA
WRITE (6,403)
WRITE (6,404) W,L,H,PM

C
C SPECIFICS
WRITE (6,405)
WRITE (6,406) WC,WA
WRITE (6,407) L1,L2
WRITE (6,408) SRC,SRA

C
C RESULTS
00330 WRITE (6,412) E
WRITE (6,413) EREV
WRITE (6,414) DECHM
WRITE (6,415) (DECHM(I),I=1,4)
WRITE (6,416) DECON
00401 FORMAT (42H1***** DESIGN SPECIFICATIONS ***** )
00402 FORMAT (114HPRESSURE = , F10.3, 4H ATM / 14H TEMPERATURE = , F10.1
1, 6H DEG K / 19H CURRENT DENSITY = , F10.2, 9H AMP/50CM /
2214 KOH CONCENTRATION = , F10.2, 7H NORMAL )
00403 FORMAT (20H0**** CELL DATA **** )
00404 FORMAT (24H0ELECTROLYTE FLOW RATE = , F10.4, 12H CC/SEC-50CM /
113H CELL WIDTH = , F10.2, 7H CM / 20H ELECTRODE HEIGHT = , F10.1,
2 3H CM / 20H MEMBRANE RESISTANCE = , F10.7, 9H OHM-CMS3 )
00405 FORMAT (20H0**** SPECIFICS **** / 23X, 17HCATHODE ANODE )
00406 FORMAT (17H ELECTROLYTE RATE , 3X, 2F10.4)
00407 FORMAT (11H CELL WIDTH , 9X, 2F10.4)
00408 FORMAT (11H SLIP RATIO , 9X, 2F10.4)
00412 FORMAT (11H0 / 29H0***** RESULTS ***** / 1H0,10X,
121H0THE CELL POTENTIAL IS , F10.4, 9H VOLTS /
223H0CONSTRUCTED AS FOLLOWS )
00417 FORMAT (11H0, 10X, 27H0REVERSIBLE CELL POTENTIAL = , F10.4,
1 6H VOLTS )
00414 FORMAT (11H0, 10X, 27H0CHEMICAL POLARIZATION = , F10.4, 6H VOLTS )
00415 FORMAT (11H0, 10X, 20H0OHMIC LOSS IN CELL = , F10.4, 9H VOLTS /
119H MADE UP AS FOLLOWS / 11H ANODE SIDE , F10.4 /
213H CATHODE SIDE ,F10.4 / 9H MEMBRANE , F10.4)
00416 FORMAT (11H0,10X, 29H0CONCENTRATION POLARIZATION = , F10.4,6H VOLTS)
RETURN
END

```

Sample Data Set

01

\$OPVAR \$END
\$RATIO \$END
\$CELL \$END

Output for this Data

***** DESIGN SPECIFICATIONS *****

PRESSURE = 1.000 ATM
TEMPERATURE = 350.0 DEG K
CURRENT DENSITY = .20 AMP/SQCM
KOH CONCENTRATION = 5.00 NORMAL

**** CELL DATA ****

ELECTROLYTE FLOW RATE = .0158 CC/SEC-SQCM
CELL WIDTH = .30 CM
ELECTRODE HEIGHT = 100.0 CM
MEMBRANE RESISTANCE = .100 OHM-CMSQ

**** SPECIFICS ****

	CATHODE	ANODE
ELECTROLYTE RATE	.0100	.0053
CELL WIDTH	.2000	.1000
SLIP RATIO	1.0000	1.0000

***** RESULTS *****

THE CELL POTENTIAL IS 1.9143 VOLTS

CONSTRUCTED AS FOLLOWS

REVERSIBLE CELL POTENTIAL = 1.1381 VOLTS

CHEMICAL POLARIZATION = .3427 VOLTS

OHMIC LOSS IN CELL = .3836 VOLTS

MADE UP AS FOLLOWS

ANODE SIDE .1212
CATHODE SIDE .2424
MEMBRANE .0200

CONCENTRATION POLARIZATION = .0003 VOLTS

Table I

Summary of Electrolysis Cell Performance

<u>Manufacturer</u>	P atm	T °C	amp/cm ²	KOH concn %	E volts	%	Size tons/day	Cost 10 ⁶ \$
Electrolyser	1	70	.16	28	2.04	74	-	-
Teledyne	6.8	82	.43	25	1.84	82	25	6
Lurgi	30	95	.19	25	1.84	82	35.7	14.2
Bamag	1	80	.25	26	1.92	78	7.85	2.67
Norsk Hydro	1	80	.15	25	1.87	81	95	35.9
Life Systems	1	93	.65	35	1.84	82	-	-
G. E.	200	82	1.08	-	1.85	81	-	-

Figure 1

EFFECT OF CURRENT DENSITY ON ELECTROLYSIS CELL POTENTIAL

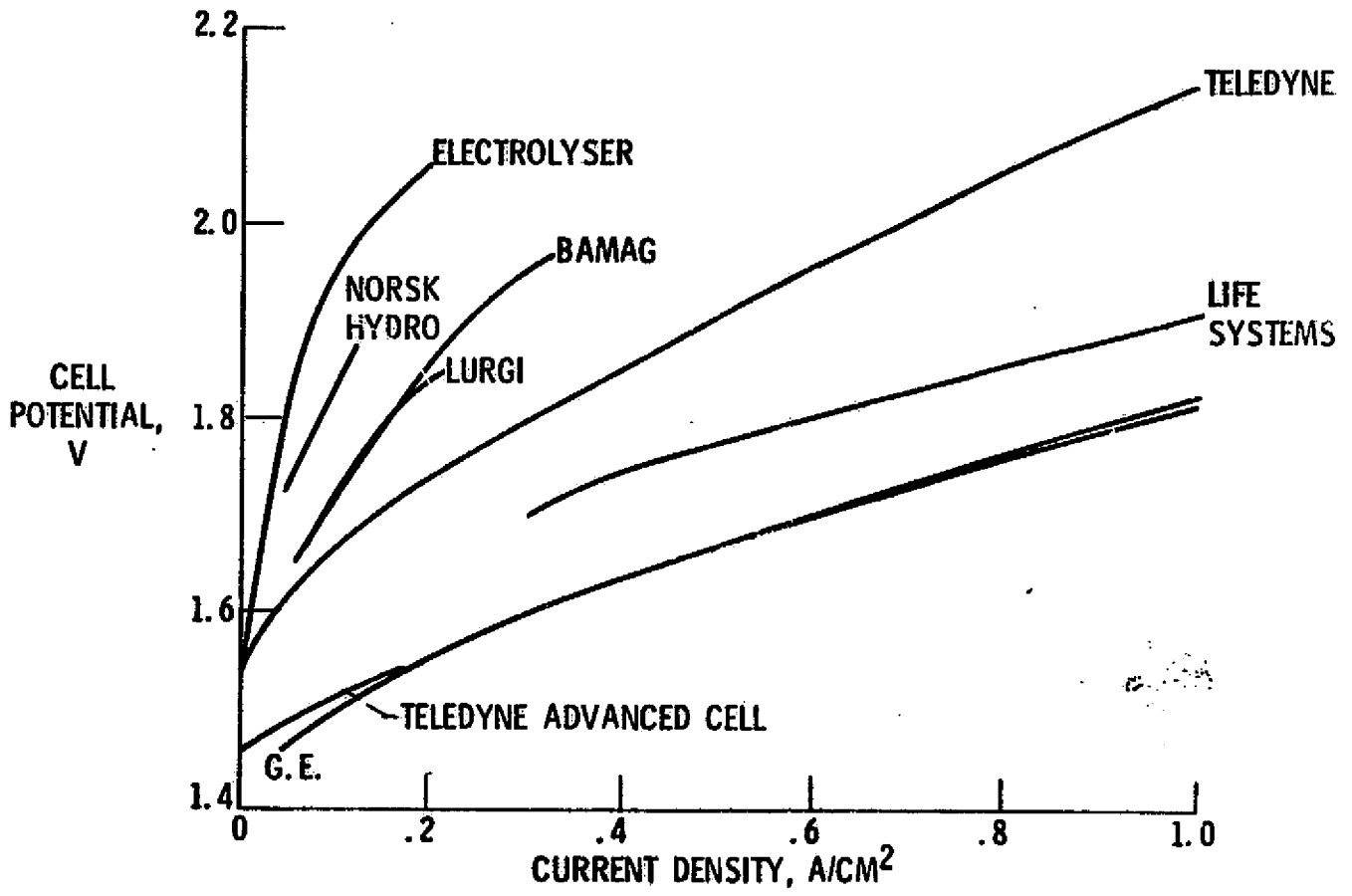


FIGURE 2

ELECTROLYSIS CELL MODEL

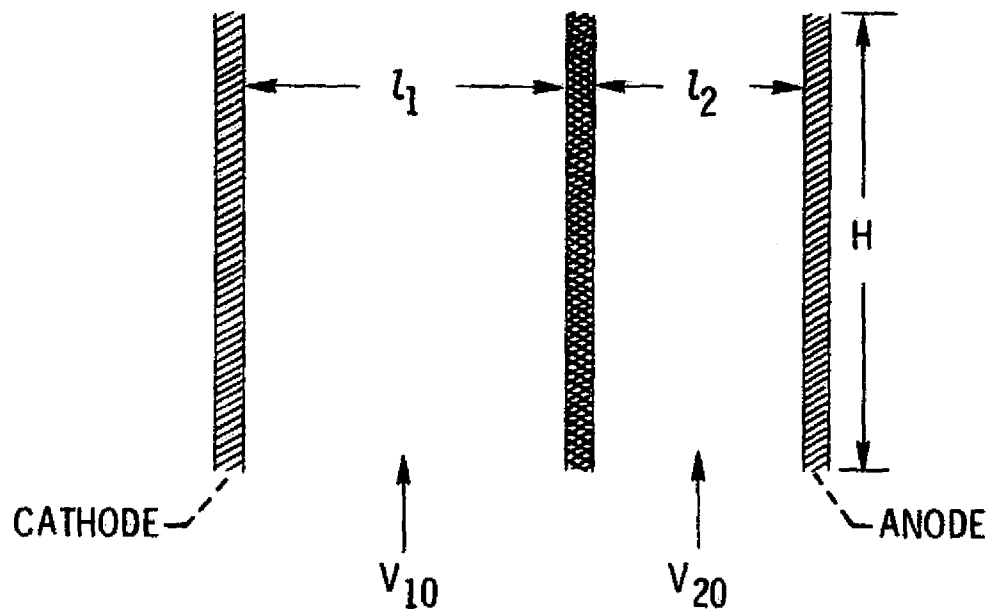


Figure 3

MODEL VERIFICATION USING COMMERCIAL CELL DATA

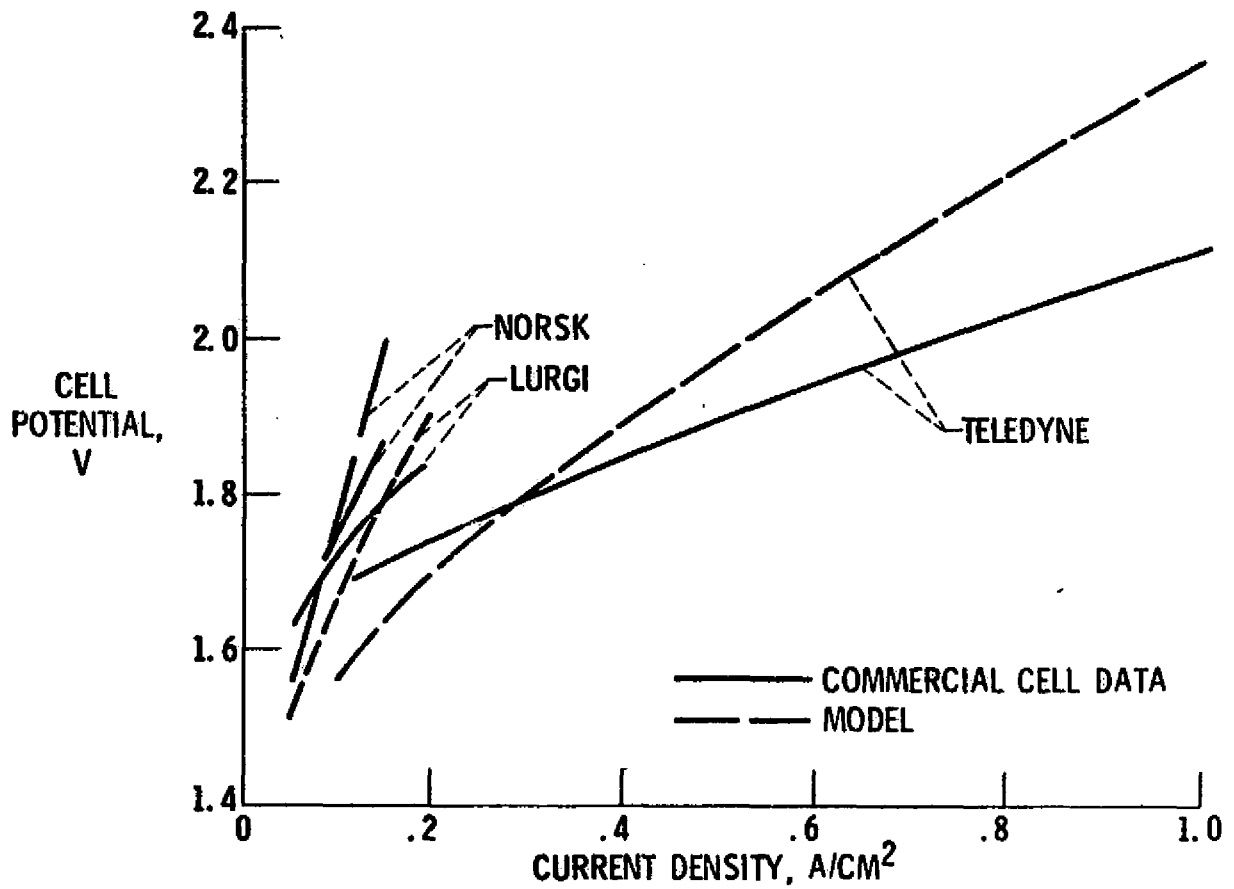


Figure 4

MODEL VERIFICATION USING RESEARCH CELL DATA
TEMP EFFECTS

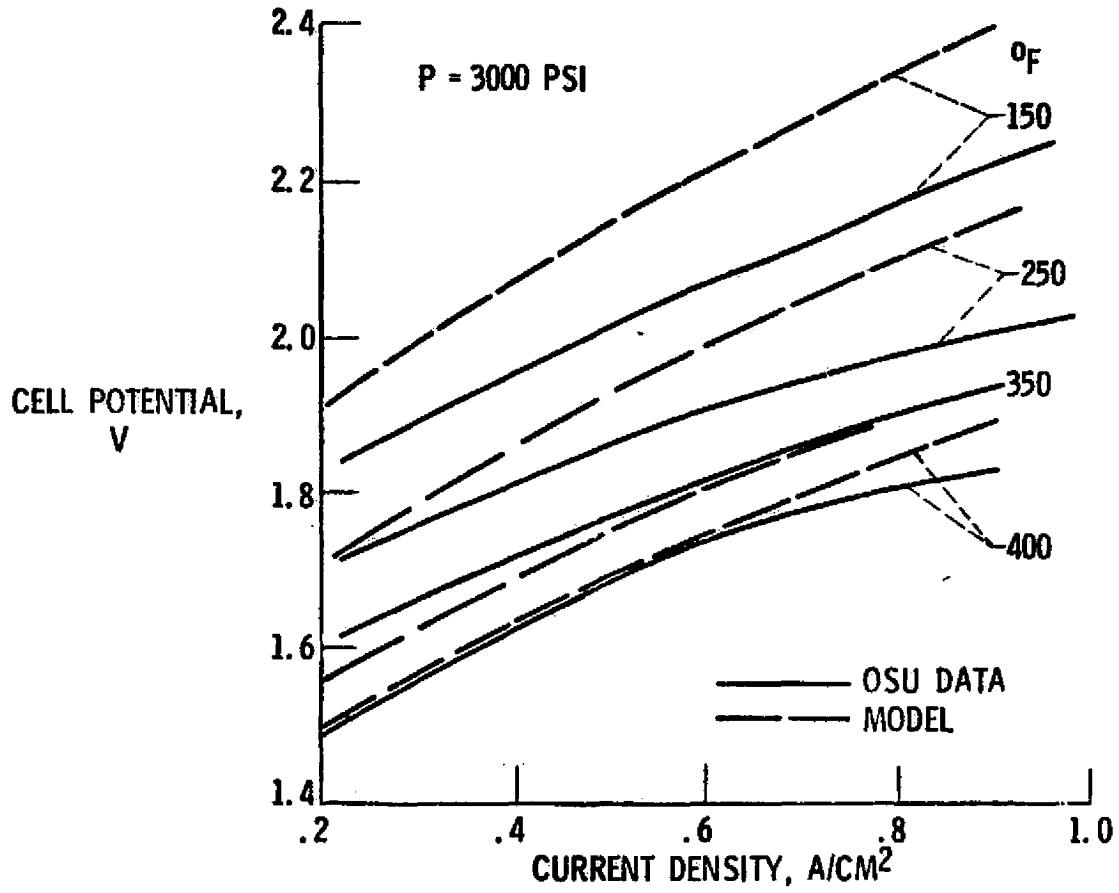


Figure 5
MODEL VERIFICATION USING RESEARCH CELL DATA
PRESSURE EFFECTS

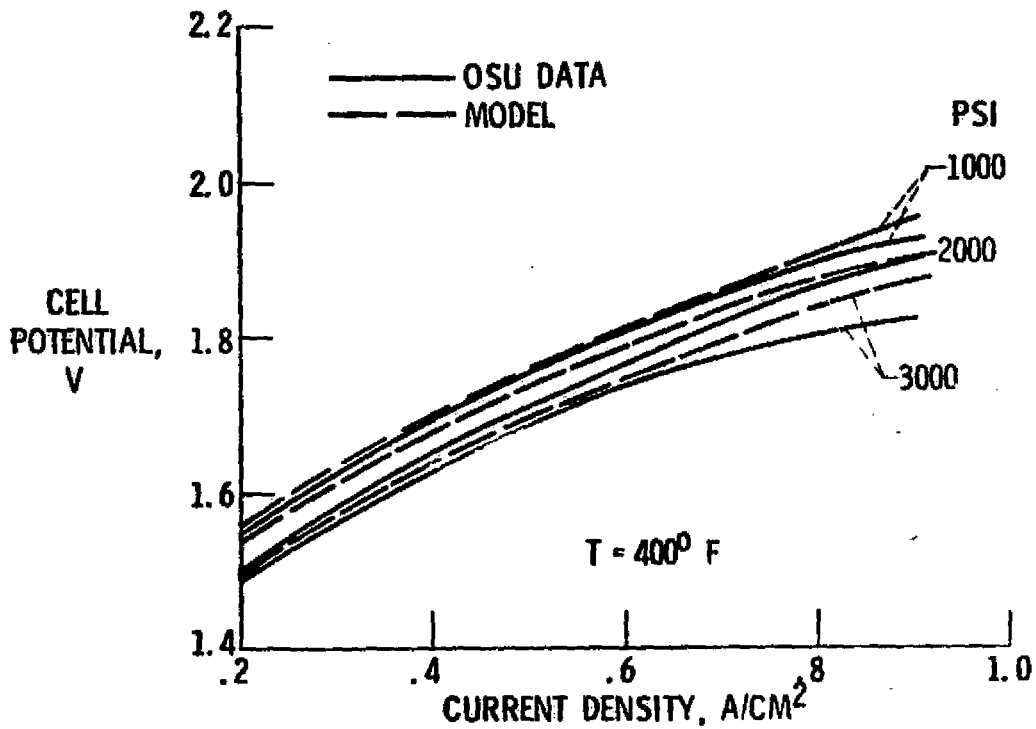


Figure 6

EFFECT OF PRESSURE ON CELL POTENTIAL

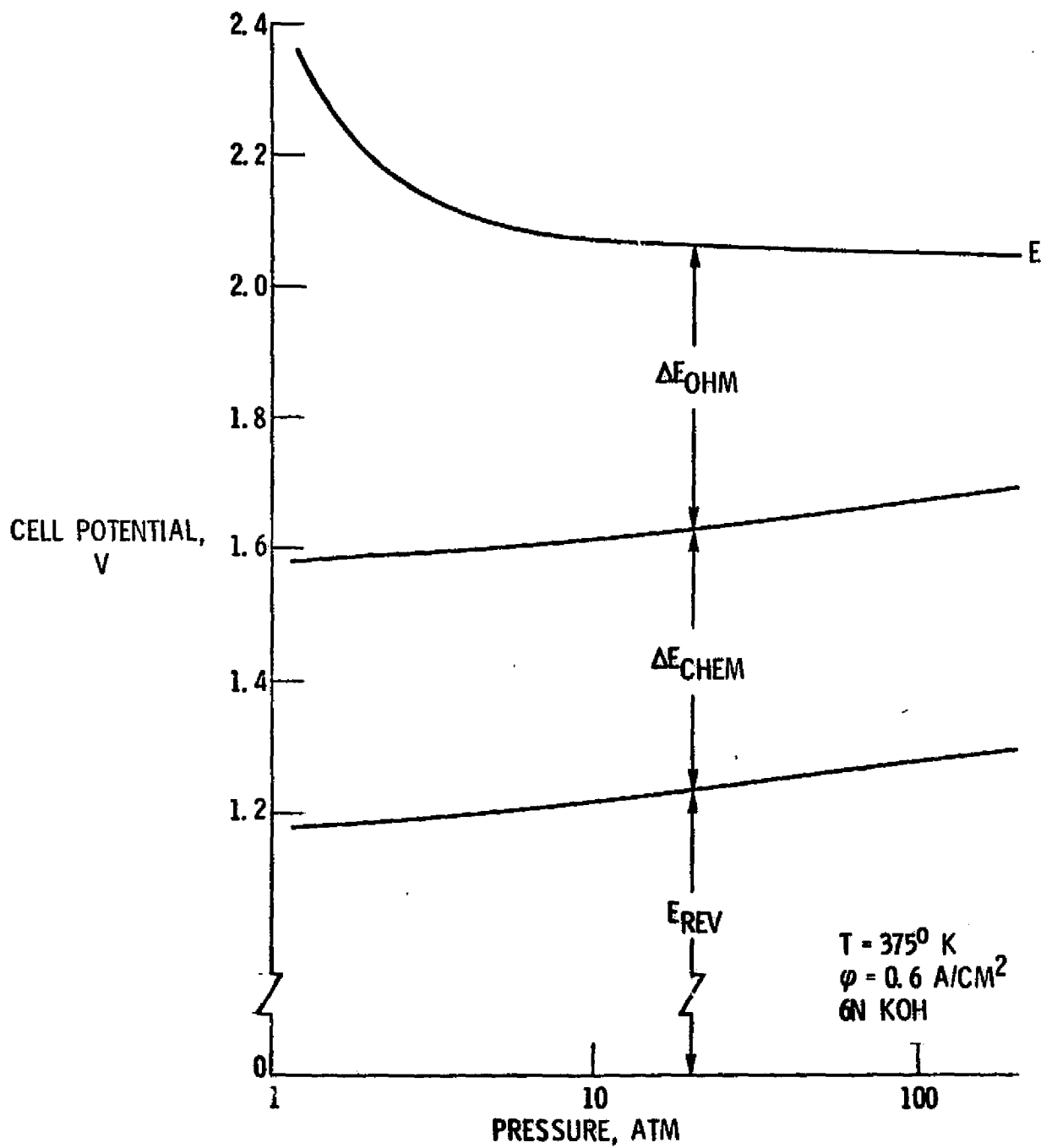


Figure 7

EFFECT OF CURRENT DENSITY ON CELL POTENTIAL

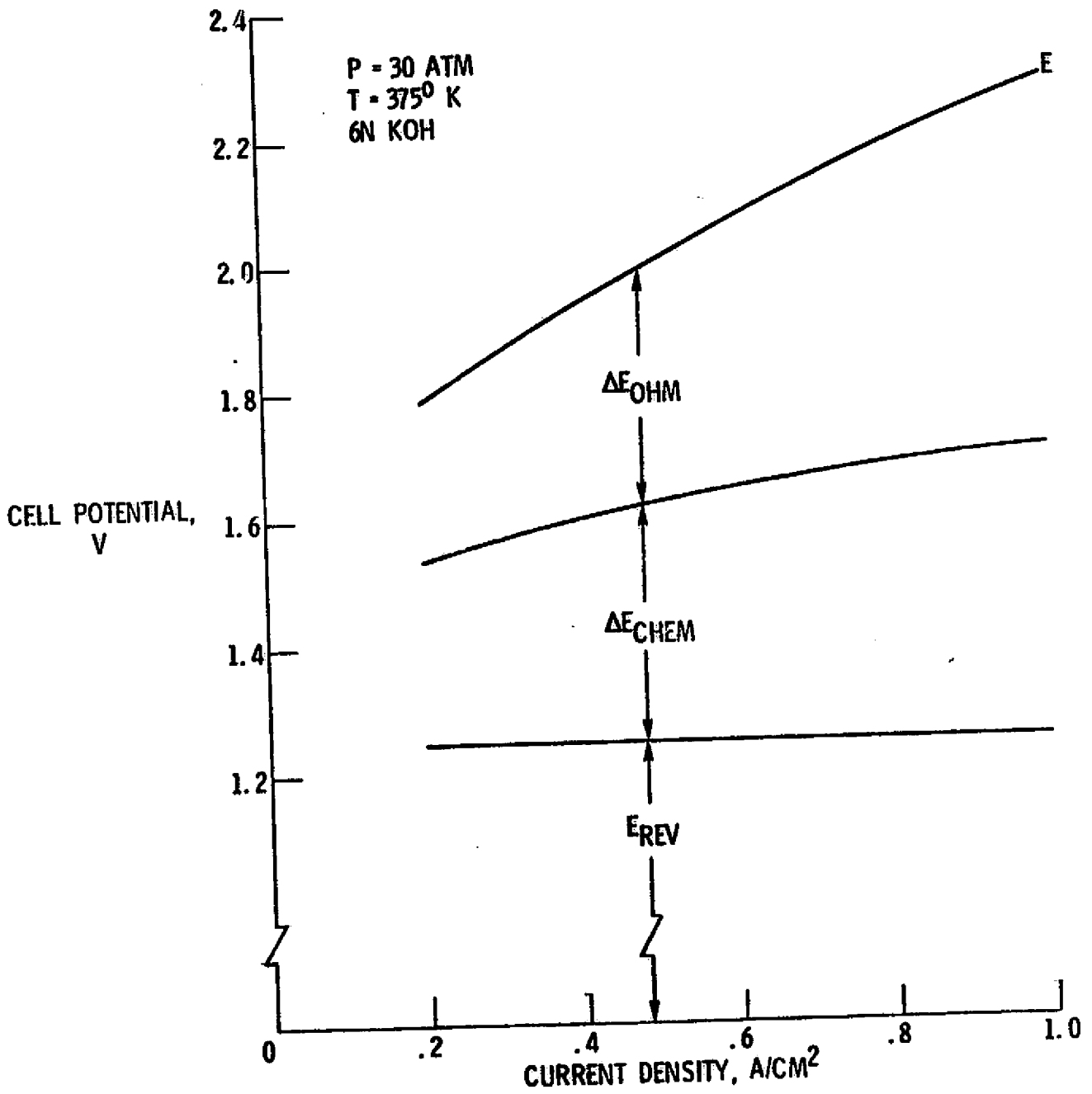


Figure 8

EFFECT OF TEMPERATURE ON CELL POTENTIAL

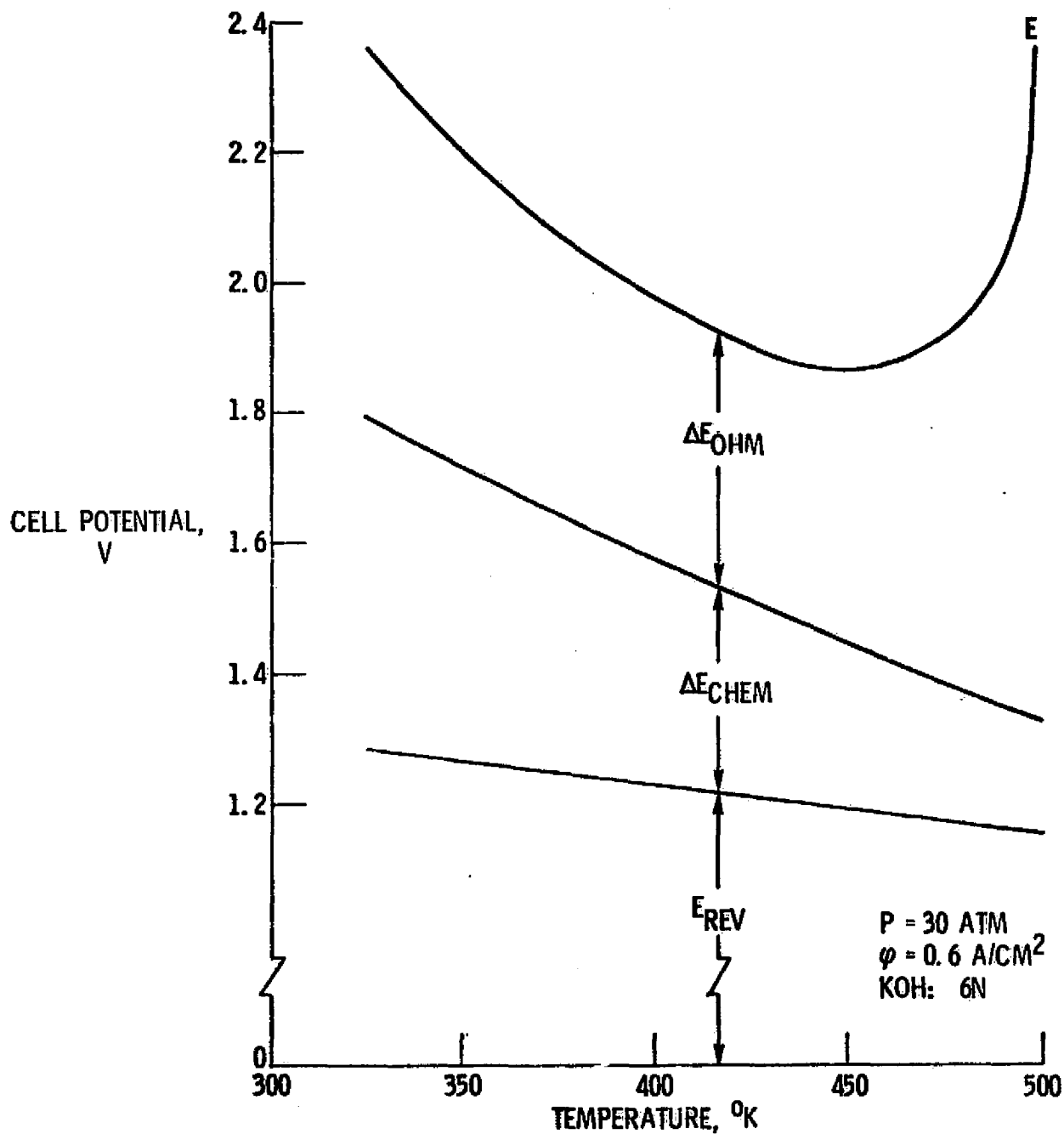


Figure 9

EFFECT OF ELECTROLYTE CONCENTRATION ON CELL POTENTIAL

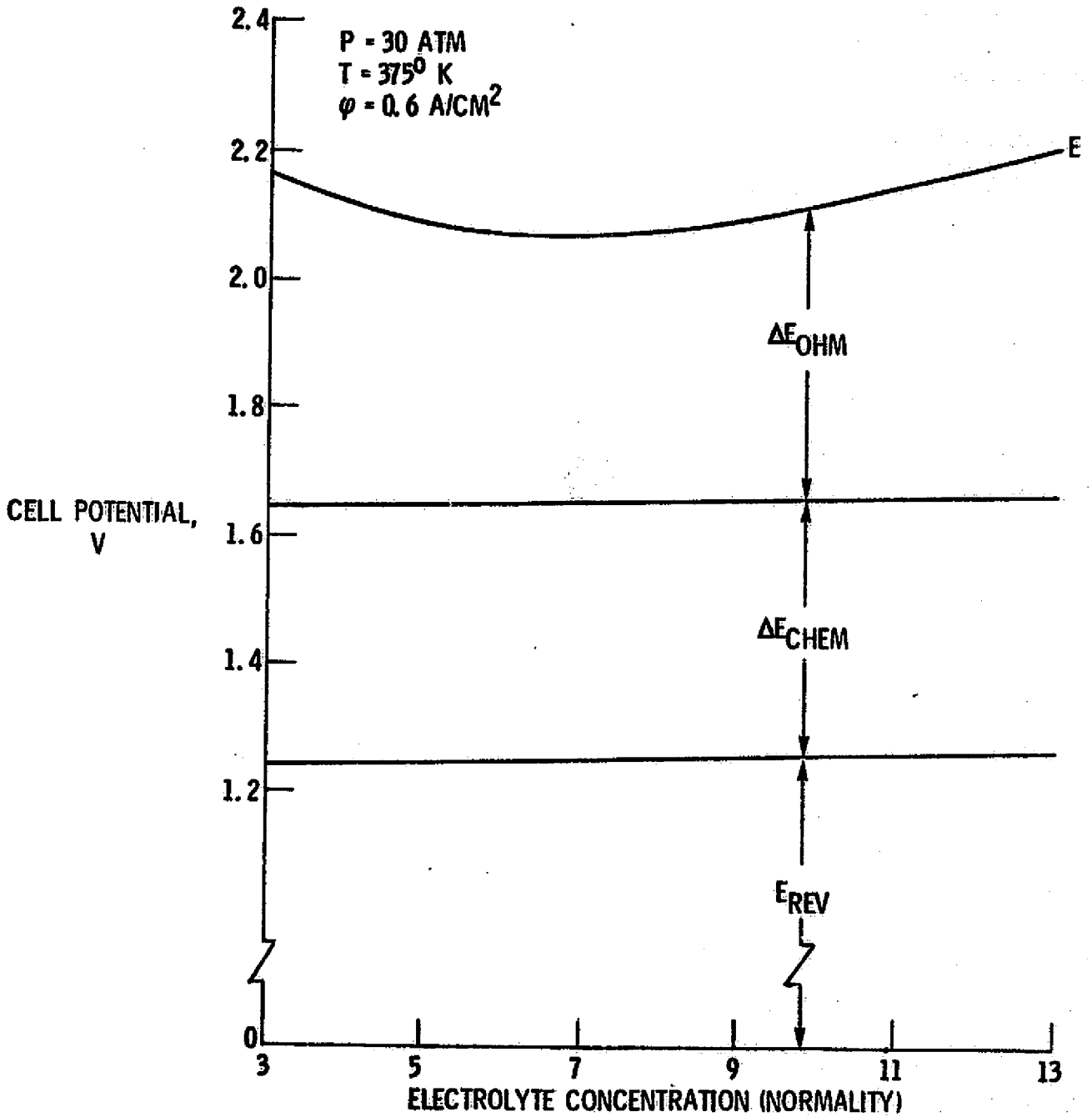


Figure 10

EFFECT OF ELECTRICAL PULSING ON ELECTROLYSIS CELL OPERATION

